Octopaminergic neurons have multiple targets in *Drosophila* larval mushroom body calyx and regulate behavioral odor discrimination

Authors

Alex D McLachlan, J Y Hilary Wong, Bo Angela Wan, Cahir J O'Kane, Marcella Montagnese, Shuo Wei Zhang, Liria M Masuda-Nakagawa*

Department of Genetics, University of Cambridge, UK

*** Correspondence to LMM-N**
lm546@cam.ac.uk
Department of Genetics
University of Cambridge
Downing Street
Cambridge, CB2 3EH
United Kingdom

Abstract

The insect mushroom bodies (MBs) are essential for associative olfactory learning, and their sensory input region, the MB calyx, is organized in discrete glomeruli, most of which receive stereotypic input from olfactory projection neurons (PNs). Odors are represented by activity of MB neurons, the Kenyon Cells (KCs) using a sparse code that allows odor discrimination during learning. Octopamine (OA) is a neurotransmitter that signals reward in associative learning and arousal, in insects including *Drosophila*. The calyx receives OA innervation from two neurons, sVUMmd1 and sVUMmx1, originating from their respective neuromeres in the suboesophageal zone (SEZ). To understand how these OA inputs might influence odor discrimination in the MBs, we analyzed their pattern of innervation of the MB calyx, their connectivity with the other neurons that innervate the calyx, and their influence on sensory discrimination during learning.

Clonal labeling of multiple single neurons showed that the two sVUM1 neurons innervated all regions of the calyx. GRASP (GFP Reconstitution Among Synaptic Partners) revealed contacts of sVUM1 neurons in the calyx with olfactory PNs, the inhibitory neuron APL, a pair of extrinsic neurons with dendrites throughout the calyx, but only few contacts with KCs. A GFP protein trap of the OA receptor Oamb, a *Drosophila* alpha-1-adrenergic receptor ortholog, localized to PN terminals in the calyx. In a behavioral odor discrimination assay, activating a set of 5 OA neurons, including the sVUM1 neurons, compromised the ability to discriminate similar odors.

Our results support a model, in which OA release from sVUM1 neurons can increase sensitivity but decrease discrimination in the olfactory learning pathway, either by modifying release from PN terminals, or interacting with the negative feedback look that comprises Kenyon cells and the APL.

Introduction

Animals need to discriminate among many sensory cues to form memories of behaviourally relevant sensory cues. Neuromodulators provide contextual meaning to sensory stimuli. In the mammalian brain, behavioural studies have shown that activity in noradrenergic systems is correlated with stimulus salience, attention, and memory formation and retrieval (reviewed by Sara, 2009; Sara and Bouret, 2012). Noradrenaline (NA) acts by affecting signal to noise/ratio and gating (reviewed by Berridge and Waterhouse, 2003), fine tuning to preferred tunes in the auditory and visual cortex (Hurley 2004), and temporal dynamics of firing in the rat piriform cortex (Bouret and Sara, 2002). Pharmacological studies have shown that NA is required for learning that involves discrimination among similar odors (Doucette et al., 2007), and adrenergic blockers affect synchronised firing of mitral cells, the second order olfactory neurons impairing similar odor discrimination (Doucette et al., 2011). NA is synthesized by relatively small numbers of neurons in the locus coeruleus in the brainstem, around 1,500 in rodents and 15,000 in primates, which innervate widely through the forebrain, including the olfactory bulb (Sara and Bouret, 2012).

Octopamine (OA) is the invertebrate functional analogue of noradrenaline (NA). OA has diverse functions such as signalling stress (Orchard et al. 1981), regulation of flight patterns (Goosey and Candy, 1980) and arousal (Stern 1999). It is also implicated in the regulation of behaviors as aggression, courtship, and higher brain functions such as learning and memory (reviewed by Verlinden 2010).

The calyx of the MBs, the sensory input region of the MBs, and a second order olfactory center, also receives OA innervation. In third instar larvae the calyx is organized in about 34 glomeruli, of which two thirds receive stereotypic innervation from olfactory projection neurons (PNs). Each KC arborizes in multiple different glomeruli, suggesting that KCs process information in a combinatorial coding manner (Masuda-Nakagawa et al., 2005), consistent with physiological data in locust showing broadly odor responsive PNs and selective KC responses to few odors (Perez-Orive et al., 2002). The calyx receives inhibitory feedback from a single inhibitory neuron, the APL, suggesting feedback inhibition as one of the mechanism to maintain the selectivity of KCs (Masuda-Nakagawa et al. 2014, Lin et al. 2014). In addition, two OA neurons innervate the larval MB calyx, sVUMmd1 and sVUMmx1, ventral unpaired medial neurons with cell bodies in the mandibular and maxillary neuromeres of the SEZ, respectively (Selcho et al., 2014). These sVUM1 neurons also innervate the olfactory neuropiles of the antennal lobe (AL)

and lateral horn. This innervation of olfactory neuropiles is conserved in other insects; dorsal unpaired median (DUM) neurons in locusts (Bräunig, 1991), and the VUMmx1, in honey bee (Schröter et al. 2007).

In appetitive associative learning in *Drosophila* and other insects, OA *Tdc2*-expressing neurons, have been considered to mediate the reward stimulus; mutants that lack tyramine beta hydroxylase, the enzyme that synthesizes OA from Tyramine, are defective in appetitive memory (Schwaerzel et al. 2003), and optogenetic stimulation of *Tdc2* neurons can substitute for sugar reward signal (Schroll et al. 2006). Stimulation of the VUMmx1 neuron can replace the unconditioned stimulus in honeybee (Hammer 1993). However (and in contrast to the honeybee work), transgenic targeting of OA neuron subsets suggest that OA mediates reward via a subset of dopaminergic neurons, rather than directly on the MBs (Burke et al. 2012).

Neuromodulators act on a variety of receptors, and pharmacological interventions do not have the cellular precision to dissect the circuit and synaptic mechanisms of stimulus-encoding and its regulation. To understand the effect of OA innervation in regulating discrimination, at the circuit level in a higher order memory center, we make use of the powerful genetic tools of *Drosophila*, in a well defined circuit, in the *Drosophila* larval MB calyx. Our objectives were to understand the innervation pattern of VUM neurons in the calyx and their synaptic partners, the localization of OA receptors in the calyx circuit, and the impact of OA calyx innervation on behavioral odor discrimination. Our data suggest that OA neurons innervate a number of calyx neuron classes but not Kenyon cells, and that activating OA neurons can affect similar odour discrimination during learning and memory, without affecting the underlying learning and memory mechanisms. Our findings therefore reveal a synaptic mechanism “gating” at the second synapse in the olfactory pathway, that has an impact on odor discrimination and learning.

Materials and Methods:

Fly Stocks. Flies were raised on standard cornmeal medium at 25°C and subjected to a 12 hour day/night cycle. Stocks used are listed in Table 1.

MultiColor FlpOut. MultiColor FlpOut was performed according to Nern et al. (2015). Females of genotype *pBPhsFlp2::PEST(attP3); +; HA_V5_FLAG_OLLAS* ("MCFO-2") were crossed with male *Tdc2-Gal4* flies. Parents were left in vials to lay eggs for 24-hour intervals. After another 24 hours, larval progeny were heat shocked at 35-37°C by immersion in a heated circulated waterbath for 15-30 minutes, thus ensuring larvae were aged 24-48 hours after egg-laying (AEL) at the time of heat shock.

GRASP. Standard GRASP was according to Gordon and Scott (2009). Reconstituted GFP was detected using rat monoclonal anti-GFP. This did not detect either of the GRASP components GFP1-10 or GFP11, when *Gal4* or *LexA* drivers were used alone. GRASP signals had to meet a criterion of occurring in two consecutive 0.5-µm confocal sections. For single cell GRASP (Karuppudurai et al., 2014), we generated larvae carrying *P{hsFLP}*12, appropriate *GAL4* and *LexA* combinations, and a recombinant chromosome with insertions *LexAOp2-IVS>stop>spGFP11::CD4::HA-T2A-Brp::mCherry (attP2), UAS-spGFP1-10::CD4,* and *UAS-HRP::CD2.* To generate labelled single cells, parents were allowed to lay eggs initially for 24-hour intervals, then for 6-hour intervals in vials containing half the amount of food. At 0-24h, 24-48h, or later at 12-18 h, 18-24 h, or 24-30 h AEL, progeny were heat shocked as above for 10-50 minutes at 37℃. Progeny were incubated from RT until dissection of non-tubby wandering third instar larvae.

Generation of an EGFP-tagged Oamb line. The *Mi{MIC}Oamb*^{MI12417} insertion in coding intron 3 of *Oamb* at 3R:20697059, (BDSC 57940; henceforth referred to as *MI12417*) was verified by PCR using primers *MI12417-5F/MiMIC-5R1* for the 5' end and *MI12417-3R/MiMIC-3F1* for the 3' end (Table 2; Supp Fig. 2). Sequencing of these PCR products and alignment with the *Drosophila* genome sequence using BLASTN (Altschul et al., 1990; https://blast.ncbi.nlm.nih.gov/) showed insertion of *MiMIC* at the recorded site of 3R 20697058-9 (Supp Figs. 3,4). The location of the *MI12417* insertion site relative to *Oamb* coding exons was determined by using Oamb-B sequences for BLASTN and TBLASTN queries of the *Drosophila* genome assembly (http://flybase.org/blast/; Supp. Fig. 5). TMHMM (Sonnhammer et al., 1998; http://www.cbs.dtu.dk/services/TMHMM/) was used to predict the amino-acid

coordinates of Oamb transmembrane (TM) domains (Supp. Fig. 6,7).

To insert an EGFP-encoding exon into the *MI12417* insertion by RMCE, we chose the splice phase-1 version of *EGFP-FlAsH-StrepII-TEV-3xFlag* plasmid (DGRC 1306; Venken et al., 2011) as recommended by the Baylor Gene Disruption Project (http://flypush.imgen.bcm.tmc.edu/pscreen/rmce/rmce.php?entry=RM00888). This was co-injected with a helper phiC31-integrase plasmid (Venken et al., 2011) by the *Drosophila* microinjection facility (Department of Genetics, University of Cambridge). Injected embryos were left to hatch into adult flies and crossed to a *y w* double balancer stock. RMCE events were identified by loss of the *MiMIC yellow*$^{+}$ marker in F1 progeny. Four PCR reactions were carried out to determine the orientation of the EGFP cassette in each recombinant *Oamb::EGFP* stock (Table 2) as described in Venken et al. (2011).

***OctβR* EGFP fusions.** For *Octβ1R* and *Octβ3R*, we used lines *Octβ1R*$^{MI05807\text{-}GFSTF.2}$ and *Octβ3R*$^{MI06217\text{-}GFSTF.1}$ (Bloomington stocks 60236 and 60245), respectively, as *Octβ1R::EGFP* and *Octβ3::EGFP* exon traps. For *Octβ2R*, we used *Mi{MIC}Octβ2R*^{MI13416} to generate *Octβ2R*$^{MI13416\text{-}GFSTF.2}$ using a similar approach as that described above for Oamb::EGFP. We also generated a second *Octβ3::EGFP* exon trap, *Octβ3R*$^{MI06217\text{-}GFSTF.0}$, in a different reading frame from Bloomington stock 60245 , to allow for the possibility of the *EGFP* exon being spliced as in transcripts *RJ* or *RK* (frame 0, with only *RJ* able to encode all seven TM domains), rather than *RF* or *RG* (frame 1). Positions of each insertion were confirmed by PCR and sequencing similarly to Oamb, using primers as described in Table 2.

Molecular methods. Genomic DNA was extracted from 15-30 flies (1-7 days after eclosion) and homogenized in 100 mM Tris-HCl, 8.5; 80 mM NaCl, (Sigma 31434); 5% Sucrose (Sigma S0389); 0.5% SDS (Sigma L4509); 50 mM Na-EDTA (Sigma ED2SS), pH 8.0. The homogenate was incubated with RNase A (Roche 10109142001) for 1 hour at 37°C followed by Proteinase K (Roche 03115887001) for 1 hour at 50°C, and purified with phenol-chloroform (Sigma 77617) and chloroform (Sigma C2432). DNA was precipitated with 0.6 volumes of isopropanol (Sigma, 59304) and washed with 75% ethanol (Sigma E7023), dried overnight at room temperature and re-suspended in 10 mM Tris-HCl pH 8.0 (Sigma T6066).

PCR reactions (20 µl) contained 0.4 µl or 1 µl genomic DNA, 1 µl of each 10 µM primer (Sigma), 2µl 10X PCR buffer (Qiagen 203203), 0.4 µl 10 µM dNTP mix (Roche 11581295001), 0.08 µl 5 U/µl HotStarTaq DNA polymerase (Qiagen 203203) and 15.1 µl or 14.5 µl milliQ water. PCR

cycling in a G-Storm Thermal Cycler (GS4) was: 15 minutes at 95°C; 40 cycles of: denaturation at 94°C for 30s, annealing at 60°C for 30s and elongation at 72°C for 1 min; and a final elongation step at 72°C for 10 minutes. PCR products were loaded with 6X DNA gel-loading dye (ThermoFisher R0611) on a 1% Agarose Gel (LifeTech 16500500; 1X TBE buffer, LifeTech 16500500) with GelRed (Biotium 41003-T) for gel electrophoresis. 100 bp DNA ladder was used as a marker (LifeTech 15628019). PCR products were purified using the Qiaquick PCR Purification Kit (Qiagen, 28104), and sequenced at the Department of Biochemistry Sequencing Facility (University of Cambridge).

Immunohistochemistry and Confocal imaging.

Third instar wandering larval brains (144-176 hours AEL) were dissected in cold PBS (Sigma P4417), fixed in 4% Formaldehyde (Polysciences 18814) / PEM buffer (0.1 M PIPES, Sigma P1851; 2 mM EGTA, Sigma E3889; 1 mM $MgSO_4$; NaOH) for 2 hours at 4°C, washed for 3x10 minutes (or 4x15 minutes) in 0.3% Triton-X (Sigma T8787) in PBS (PBT) and incubated in 10% NGS (Normal goat serum; Vector Labs S-1000) in 0.3% PBT for 1 hour at room temperature. Brains were incubated in primary antibody in 10% NGS-0.3% PBT at 4°C for 2-3 days on a mini disk rotor (Biocraft, BC-710), washed for 3x15 minutes with 0.3% PBT and further incubated in secondary antibody in 10% NGS at 4°C for 2-3 days again on the mini disk rotor. Brains were finally washed 1x15 minutes with PBT, followed by 3x10 minutes with PBS, and left in 50% Glycerol/PBS at 4°C for at least one overnight prior to imaging.

Primary and secondary antibodies are listed in Table 3. Brains were incubated in primary antibody at 4°C for 2-3 nights, washed three times in PBT for 15-minutes, and incubated in secondary antibody for 2-3 more nights. To reduce background with the polyclonal chicken anti-GFP (Abcam, Ab13970), it was pre-incubated with *MI12417* larval brains which do not express GFP. Fifty *MI12417* larval brains were incubated in 1:20 chicken anti-GFP in 10% NGS in 0.3% PBT at 4°C for overnight. A further 50 *MI12417* larval brains were added and further incubated at 4°C over 2 nights. Mounting and orientation of brains for image acquisition was as described in supplemental information in Masuda-Nakagawa et al. (2009). Imaging was carried out using a Zeiss LSM710 Confocal Microscope with a 40X NA1.3 oil objective. Images were processed using ImageJ software (https://imagej.nih.gov/ij/download.html).

Behavioral assay.

<u>Larval culture.</u> Males of genotype *w; Tdc2-LexA; GMR34A11-GAL4/TM6B* were crossed to females of genotype *Tub84B(FRT-GAL80)1, w; LexAop-FLP; UAS-Chrimson::mVenus/TM6B*

to generate F1 larvae in which *UAS-Chrimson::mVenus* could be expressed only in cells expressing both *Tdc2-LexA* and *GMR34A11-GAL4*, in which LexA-dependent *FLP* expression had removed the GAL4 inhibitor GAL80. Larvae were allowed to develop in food vials containing 0.2 mM all-trans-retinal, in the dark at 21 degrees. For both the retinal and non-retinal food vials, transfer of adults into new vials happens both in the morning and in the evening, to then collect them after 108-120 hours in the case of non-retinal vials at 25°C, and after 132-144 hours for those kept in retinal vials at 23°C.

Behavioral arena. Agarose petri dishes were prepared the day before use, by using 100 ml of distilled water with 0.9% agarose (Sigma A9539). Fructose petri dishes were prepared the day before use, by using the same solution containing 35% fructose (SIGMA-47740). Petri dishes had perforated lids, to facilitate creation of odorant gradients within the dish, by sucking air from a benchtop fume extractor (Sentry Air Systems (SAS), SS-200-WSL) at the back of the assay platform. Odorants were diluted in 10-µl volumes of paraffin oil (Sigma-Aldrich 76235), held in custom-built Teflon containers with pierced lids (7 holes), on the surface of agarose plates.

Light apparatus. The light apparatus contained a BK Precision pulse generator attached to a DC power pack, driving amber light LEDs (591 nm), constructed as described by deVries and Clandinin (2013), by the Psychology Department workshop of the University of Cambridge. One cycle of pulses consisted of 10-ms pulses at 10Hz for 30s, followed by 30s without pulses. This cycle was repeated 5 times, making a conditioning step of 5 minutes. This pulse frequency and width were chosen to replicate the activity of the only recorded sVUM1 neuron, the honeybee sVUMmx1, when activated by a sucrose reward (Hammer et al., 1993).

Behavior conditioning. Third-instar larvae were collected from vials using a metal sieve, and washed with tap water. Larvae were washed twice by transferring through a drop of water, and then placed on the conditioning agarose plate (35% fructose). A Teflon container with 10 µl of odour A to be reinforced was placed on the left side, and another containing paraffin oil (neutral) symmetrically on the right side, at positions marked on a black background, used to facilitate visualization of the larvae (Fig. 1). Larvae were conditioned on the fructose plate with odor A for 5 minutes under weak blue light. Larvae were then transferred a water droplet using a brush, and again to a second water droplet to ensure no fructose traces remained, and then to an agarose plate lacking fructose, on which a Teflon container with 10 µl of odour B (non-reinforced) was placed on the left side and a container with paraffin oil (neutral) on the right

side. Larvae were conditioned for 5 minutes under weak blue light as above. This conditioning procedure on both plates was repeated for three cycles. For experiments using activation of OA neurons, the entire conditioning cycles were carried out under amber light (Fig. 1).

Odor dilutions. To avoid bias based on innate preferences of odors, odor concentrations were balanced to achieve a response index of around zero. Dilutions of ethyl acetate (EA) at 1:2000 and pentyl acetate (PA) at 1:500 were used. The dissimilar odor pair was ethyl acetate (EA) (Sigma-Aldrich, cat no. 319902) diluted 1:2000, and pentyl acetate (PA) (Sigma-Aldrich, cat no. 109584) diluted 1:500. The similar odor pair was mixtures of EA and PA at dilutions of 1:2000, and 1:500, respectively, at proportions of 1:4 EA:PA, and 4:1 of EA:PA.

Testing. Larvae were tested by placing them on an agarose plate carrying a container with odour A on one side, and a container with odour B on the other. Test was under blue light for 5 minutes. Larvae were counted on the side of odour A (conditioned), odour B (unconditioned) or in the neutral zone in the middle. In some experiments, larvae were transferred during the above procedures under white fluorescent ceiling lighting rather than weak blue light, but we detected no difference in learning scores between these conditions using ANOVA, as described in the Results section. Response Index (PI) was calculated as:

$$PI = \frac{N_{conditioned} - N_{unconditioned}}{N_{Total}}$$

N conditioned: larvae on the side of the conditioned odor.

N unconditioned: larvae on the side of the unconditioned odor.

N Total: larvae on the side of conditioned odor, unconditioned odor, and the middle zone.

Learning Index (LI) was calculated after both a conditioning with odour A and a reciprocal conditioning with odor B (with a different sample of larvae), using the formula:

$$LI = \frac{PI_A - PI_B}{2}$$

Statistical analysis. Planned comparisons were performed using t-tests. A four-factor ANOVA using SPSS software was used to test whether learning index was affected by food type (retinal vs. non-retinal), light (blue vs. amber), odour pairs (similar pair vs. dissimilar pair), or experimenter (either of two).

Results

sVUM1 neurons in the calyx and their polarity.

Two OA neurons innervate throughout the calyx without obvious regional preference. The larval calyx is innervated by two classes of OA neurons, sVUMmd1, and sVUMmx1, originating from the mandibular and maxillary neuromeres, respectively, in the subesophageal zone (SEZ), and labeled by the *Tdc2-GAL4* line (Selcho et al. 2010; 2014). To visualize the innervation pattern of both sVUM1 neurons in the calyx together, we used the Multicolor FlpOut technique (Nern et al. 2015). Flies of genotype *pBPhsFlp2::PEST(attP3); HA_V5_FLAG_OLLAS* were crossed to flies of *Tdc2-Gal4*, and single cell clones were generated by heat shock. Each sVUM1 neuron ramified throughout the calyx, and we only ever found a single sVUMmd1 or sVUMmx1 neuron labeled. When both sVUM1 neurons were labeled, they ramified through the calyx in a non-overlapping pattern, without obvious regional preference (Fig. 2).

OA neurons are presynaptic in the calyx. To visualize the polarity of the calyx-innervating sVUM1 neurons, we used *Tdc2-GAL4* to express either plasma membrane, presynaptic or dendritic markers (Fig. 3). The sVUM1 projections visualized by the plasma membrane marker CD4::tdTom showed dense ramification throughout the calyx, with bouton-like enlargements among glomeruli and in the core of the calyx (Fig. 3A). These enlargements contained OA, and were therefore presynaptic boutons; we observed 89 ± 7 (n= 12) OA-positive boutons per calyx. The presynaptic nature of the *Tdc2-GAL4*-expressing calyx boutons was further supported by the localization of the presynaptic markers nSyb::GFP (Fig. 3A) and Syt::GFP (Fig. 3B) in puncta throughout the calyx in these neurons, prominently between glomeruli or in the non-glomerular core of the calyx. The dendritic marker DenMark::mCherry is not detectable in the calyx (Fig. 3B), although it is strongly localized in the SEZ region (Fig. 3C), which may include other Tdc2-GAL4-expressing neurons as well as the sVUM1 neurons.

Identifying calyx OA neuron partners by GRASP

To visualise synaptic contacts between sVUM1 neurons and other calyx neurons, we used *Tdc2-LexA* or *Tdc2-GAL4*, along with *GAL4* or *LexA* lines expressing in other calyx neurons, to drive the expression of the GRASP constructs *LexAop-CD4::spGFP11 and UAS-CD4::spGFP1-10* (Fig. 4). We labeled olfactory PNs using *NP225-GAL4* (Tanaka et al., 2009), and KCs using either *MB247-LexA* (Pitman et al., 2011), or either of two lines, *H275-IT.GAL4* or *H500-IT.GAL4* Supplementary Fig. 1), that we generated by mobilization of an InSITE enhancer trap element (Gohl et al., 2011). We also tested for GRASP between sVUM1 neurons

and two other classes of extrinsic calyx neurons. First, we labeled the larval APL using *NP2361-GAL4* (Masuda-Nakagawa et al., 2014), Second, the “Odd” class of neurons shows dendritic arborizations throughout the calyx, with presynaptic terminals in the vicinity of the MB lobes (Slater et al., 2015), an appear to be the same as those designated as MBON-a1 and MBON-a2 by Eichler et al (2017); we identified a *GAL4* line, *OK263-GAL4*, which expresses in these neurons.

GRASP fluorescence. We detected GRASP using GFP fluorescence as widely distributed puncta in the calyx, suggestive of specific synaptic connections, between the sVUM1 neurons on the one hand, and PNs, the APL, and the Odd neurons on the other. However, we detected only fainter GRASP signal between the sVUM1 neurons and KCs, which mostly ran along dispersed tracts in the calyx (presumably sVUM1 axonal tracts that may be surrounded by the large number of KC dendrites), with only few puncta that were not substantially brighter than the axonal signals (Fig. 4A). These findings suggest that the sVUM1 neurons may form synapses with PNs, the APL and the Odd neurons, but fewer and weaker synaptic connections with KCs.

To test whether GRASP signals represented synaptic contacts of the sVUM1 neurons, we also immunolabelled brains with anti-OA. GRASP signals were identified, using a criterion that each GRASP signal was observed in 2 consecutive confocal sections, and discounting occasional GFP-positive axonal tracts that were negative for OA.

OA termini synapse with PNs. Using *Tdc2-LexA* and *NP225-GAL4* to express the GRASP constructs, we found GRASP signal at 49±3% of 80±4 (n=5) OA-positive boutons. OA-positive GRASP signals (Fig. 4B) were found in the core of the calyx away from glomeruli, in interglomerular spaces, and along the periphery of glomeruli. They are likely contacts between sVUM1 termini and PN axons. Not all GFP overlapped with OA, 6.2±2 GFP (n=5) signals; 13.5% (n=5) of total GRASP signals did not co-localised with OA. Therefore PNs are likely postsynaptic to sVUM1 neurons, on their axonal or presynaptic processes, making axon-axon synapses.

OA termini synapse with the APL. Using *Tdc2-LexA* and *NP2361-GAL4* to express the GRASP constructs, we found GRASP signal at 77±4% of 74±12 (n=4) OA terminals, indicating that sVUM1 neurons are presynaptic to the larval APL. Most of these GRASP signals were found between glomeruli, and more abundant towards the ventral calyx (Fig. 4C top panels).

Around 28.3 ± 1 GFP signals, 32.8 % ± 2.6 (n=3) GRASP signals, did not overlap with OA, and therefore do not represent synapses of the sVUM1 neurons onto the APL. Some of these appear to be tracts that lead to OA positive spots, rather than the characteristic round shape of synaptic GRASP signals, and might therefore be due to proximity of the sVUM1 axons with APL axons. Others could be due to synapses of the APL onto OA neuron axons. GABA labeling of brains of the same genotype, showed some GABA termini in close proximity to GRASP (Fig. 4C, bottom panels), suggesting that some contacts between APL and sVUM1 neurons could potentially be inputs from APL terminals onto the sVUM1 neurons. Labeling of Tdc2-GAL4>mCD8::GFP calyces with anti-GABA also showed some apposition of sVUM1 boutons to GABAergic termini of the APL (Fig. 4D).

OA termini synapse with Odd neurons in the calyx. Using *Tdc2-LexA* and *OK263-GAL4* to express the GRASP constructs, we found GRASP signals at 51 ± 0.3 % of 123 ± 4.2 (n=3) OA labeled boutons. There were OA spots that were apposed to GFP (Fig. 4E).

OA neurons do not contact KCs in the calyx. To visualize potential contacts between KCs and sVUM1 neurons, we used either *Tdc2-Gal4* and *MB247-LexA*, or *Tdc2-LexA* along with either *H275-IT.GAL4* or *H500-IT.GAL4* to drive expression of the GRASP constructs. Only very occasional spots were observed, but these did not overlap with OA immunolabeling (Fig. 4F), implying that they were not synaptic contacts.

Single cell GRASP. While the above GRASP experiments reveal the partners of the sVUM1 neurons in the calyx, they do not reveal whether the sVUMmd1 and sVUMmx1 have different partners. We therefore performed single-cell GRASP in *Tdc2-LexA*-expressing neurons to label the contacts of each sVUM1 randomly, and used Brp::mCherry as a presynaptic marker to verify whether GRASP signals have a synaptic localisation. We distinguished the two sVUM1 neurons by the positions of their cell bodies in the SEZ, using local neuropil landmarks revealed by anti-Dlg labelling (Fig. 5A), and using single cell clones, we could identify sVUMmd1 and sVUMmx1 individually (Fig. 5B).

GRASP signals were detected between the larval APL and both sVUMmd1 and sVUMmx1 (Fig. 5C), and similarly between the *odd*-expressing neurons and both sVUMmd1 and sVUMmx1 (Fig. 5D). Compared to standard GRASP, single cell GRASP signals were fewer, but clearly present and overlapping with the presynaptic marker Brp::mCherry. (Fig. 5D).

Consistent with the results of standard GRASP (Fig. 4D), we detected no single-cell GRASP signals between KCs and either sVUMmd1 or sVUMmx1 (unpublished data). Therefore both sVUM1 neurons appeared to have similar targets in the calyx, and may differ mainly by their inputs in the SEZ.

Localization of a genomic Oamb::GFP fusion in PN terminals in calyx

To further understand the OA circuitry in the calyx, we investigated the localization of OA receptors in the calyx. *Drosophila* has a number of OA receptor classes defined both by sequence comparisons and pharmacology. Oamb, an α-adrenergic receptor homolog, is enriched in the MBs (Han et al., 1998). *Drosophila* also has three OctβR receptors, which stimulate cAMP levels (Maqueira et al., 2005, Balfanz et al., 2005).

To detect the expression and subcellular localization of Oamb, we used recombinase-mediated cassette exchange (RMCE) with a MiMIC insertion (Venken et al., 2011), *MI12417*, in the third coding-region intron of *Oamb*, to tag endogenous *Oamb* with an exonic *EGFP-FlAsH-StrepII-TEV-3xFlag* fusion (Supp Figs. 2-5). Insertion of an EGFP-encoding exon here should tag all known splice variants of the Oamb protein in their third cytoplasmic loop, downstream of transmembrane (TM) domain 5 (Supp. Fig. 6,7); this includes the alternative TM6-TM7 regions encoded by two alternative groups of C-terminal exons (Supp Figs 5-7). Therefore, a protein trap generated from the *MI12417* insertion will not disrupt any transmembrane domains.

Six recombinant *Oamb::EGFP* stocks were recovered with the EGFP-encoding exon inserted in the same orientation as the *Oamb* transcript (Supp Fig. 8). One of these was designated as *Mi{PT-GFSTF.1}Oamb*$^{MI12417\text{-}GFSTF.1}$, or *Oamb(MI12417)::EGFP.1* or *Oamb::EGFP* for short. Both the original *MI12417 MiMIC* insertion, and *Oamb(MI12417)::EGFP* stocks were homozygous infertile, as expected from the egg-laying defects of *Oamb* mutants (Deady and Sun, 2015), suggesting that the Oamb::EGFP fusion might not be a functional Oamb protein.

However, Oamb::EGFP was localized to glomeruli in the larval calyx (Fig. 6), implying that the protein folded normally and was not degraded by the ER unfolded protein response. Expression of *UAS-RFP* in the olfactory PN line *NP225-GAL4* showed localization of Oamb::EGFP in all PN termini labeled with the GAL4 line, as well as in some calyx glomeruli not labeled by *NP225-GAL4*, which may be sites of non-olfactory sensory input (Fig. 6). The restriction of Oamb::EGFP to specific glomeruli implies that it is unlikely to be expressed in KC dendrites in the calyx, which arborize through all glomeruli. We also found no overlap of

Oamb::EGFP with GABAergic APL terminals in the calyx (Fig. 6B), implying that it was not expressed in the larval APL. *OK263-GAL4* calyx projections also showed little or no overlap with Oamb::EGFP (Fig. 6C), suggesting that Oamb is not expressed in the Odd neuron calyx dendrites.

We found no detectable localization of GFP-tagged DmOctβR receptors to the calyx (data not shown). Octβ1R::EGFP (*CG6919*) was expressed weakly in a few ventral and medial AL glomeruli, but was not detectable in the calyx. Octβ2R::EGFP (*CG6989*), was not detectable in either the calyx or AL, although it was expressed in a number of adjacent cell bodies that did not colocalize with PNs as labeled by *NP225-GAL4* driving RFP expression. We could not detect any expression of Octβ3R::EGFP.

Activation of an OA neuron subset including sVUM1 neurons impairs behavioral odor discrimination.

Since the calyx is a site where MB neurons integrate sensory information that comprises conditioned stimuli, we reasoned that modulating the processing of this information might affect the ability of the brain to discriminate among conditioned stimuli while learning, but without affecting its underlying learning ability. Therefore, to test whether OA innervation of the calyx affected odor discrimination during learning, we developed an assay that could distinguish odor discrimination assay from learning ability. The rationale of this assay was developed in the honeybee by Stopfer et al. (1997); molecularly similar odors are more difficult to discriminate than molecularly dissimilar odors, giving a measure of discriminability. In this case similar odor pairs are generated by varying the proportions of two dissimilar odors in two different odor mixes. By combining odor choice with an appetitive learning paradigm (Scherer et al. 2003), we tested the effect on behavioral odor discrimination of optogenetic activation of OA neurons in third instar larvae, using the long-wavelength absorbing channelrhodopsin, CsChrimson (Klapoetke et al., 2013).

Since we did not have *GAL4* or *LexA* drivers specific for sVUM1 neurons, we used an intersectional approach to restrict the expression of CsChrimson to a small subset of OA neurons including the sVUM1 neurons. We could use *LexAop-FLP* and a *GAL80* cassette flanked by two *FRT* sites to express *UAS-CsChrimson* only in neurons that expressed both *GMR34A11-GAL4* (which labels some VUM neurons in addition to non-OA neurons), and *Tdc2-LexA*. We thus expressed CsChrimson in only five OA neurons in the SEZ of the larval brain: two (1.8 ± 0.39 (n=12)) in the mandibular neuromere (including sVUMmd1), two (2 ± 0.43 (n=12)) in the maxillary neuromere (including sVUMmx1), and one (1 ± 0 (n=12)) in the labial

neuromere (Fig. 7). The second neuron labeled in each neuromere could be sVUM2 or sVUM3, however, sVUM1 neurons are the only neurons of this subset to innervate the AL and calyces.

Activation of these OA neurons, during conditioning but not during testing, had no effect on the ability of larvae in an appetitive learning assay using dissimilar odors, but nearly abolished their ability to learn using similar odors, implying that their odor discrimination is affected but not their underlying learning ability (Fig. 7).

Discussion

At neural level, the process of formation and retrieval of memory, requires the binding of contextual, environmental information, with sensory information that act as predictors of objects and events. Behavioral studies combined with electrophysiological recordings and pharmacological interventions have identified the neuromodulator noradrenalin as the carrier of stimulus novelty, or salience, and is involved in attentional signaling that switches network activity for behavioral changes (Sara, 2009; Sara and Bouret, 2012), Likewise in insects, the neuromodulator OA, structurally and functionally analogous to noradrenalin, was identified and electrophysiological studies combined with pharmacological interventions have suggested a role in gating, e.g making subthreshold weak signals detectable, by changing synaptic transmission at the level of sensory receptors, and primary sensory afferents (e.g. Bräunig and Eder, 1998; Widmer, 2005). However, its role in memory formation and retrieval, at the neural circuitry level remains obscure.

This work aimed to dissecting the neural and molecular circuitry of OA signaling in sensory processing at a higher brain center. The calyx of the MBs in insects, are the sensory input region of the MBs, where odor processing for learning takes place. Afferent PNs carry olfactory input, and KCs are postsynaptic to PNs. The calyx receives regulatory input from a feedback inhibitory neuron, APL, and OA innervation from sVUM1 neurons that originate in the SEZ , both in flies and larvae (Busch et al. 2009; Selcho et al., 2014).

Anatomy

Two OA originating in the SEZ, sVUMmd1 and sVUM mx1, innervate throughout the calyx of the MBs, in a non-overlapping pattern, Both neurons innervate the same brain neuropiles, with presynaptic processes in the antennal lobe and extensive presynaptic boutons in the MB calyces, and postsynaptic processes in the SEZ. This polarity is consistent with that described for *Tdc2*-expressing neurons in adult flies (Busch et al. 2009). The innervation pattern closely resembles that of VUMmx1 in honeybee (Hammer 1993) and the OA-VUMa2 neurons in adult *Drosophila* (Busch et al. 2009). A connectomic analysis of a six-hour first-instar larva has revealed two neurons, OAN-a1 and OAN-a2, with the same basic innervation pattern but with a much more restricted ramification in the calyx than we observe here, suggesting that the connectivity of these neurons at a six-hour first instar stage is not yet mature, and implying that any behavioural modulation that they mediate is also not yet mature (Eichler et al. 2017).

GRASP analysis and receptor expression

From GRASP analysis we could detect few if any contacts of sVUM1 neurons with KCs, but abundant contacts with PNs, APL and Odd neurons, suggesting that context-dependent signaling though OA affects MB activity by affecting its inputs and how they are processed, rather than directly on KC dendrites. Our single cell GRASP analysis suggests that sVUMmd1 and sVUMmx1 neurons have qualitatively similar contacts on partners APL and the Odd neurons, and that they therefore differ principally in the source of their inputs in the SEZ, rather than in their effects in the calyx.

The OAN-a1 and OAN-a2 connectomics analysis of Eichler et al. (2017) show less than half the number of presynaptic sites (36 for the left brain, and 48 for the right brain) compared to the numbers we counted (89 ± 7 [n=12] OA-positive boutons per calyx); their drawings of OAN-1a and OAN-a2 also suggest less ramification of these neurons in first instar than we find in third instar. They also report that the main postsynaptic partner for OAN-a1 and OAN-a2 are KCs, while we did not observe prominent connectivity with KCs, in our GRASP analysis, using a number of different GAL4/LexA combinations. These observations suggest that the final larval connections are not yet established at a 6-hour first instar stage, and perhaps that not all connections at the earlier stage are permanent.

The APL appears to be postsynaptic to OA neurons. Since the APL responds to KC output in the lobes and mediates a negative feeback loop that may can potentially both limit the duration of KC activity and improve their odor discrimination (Masuda-Nakagawa et al., 2014; Lin et al., 2014), OA signals from the sVUM1 neurons could be regulating this feedback loop. This could provide a mechanism of increasing signal-to-noise ratio, in a context dependent manner, by sharpening odor representations in the calyx via APL inhibitory feedback. In mammalian olfactory bulb, gating of mitral cell (equivalent to PN) activity has been proposed, mediated by decreasing the excitation of inhibitory granule cells (Ciombor et al., 1999, Hurley et al., 2004). Since some proximity of GRASP to GABA termini was also observed, there could be bidirectional signaling between sVUM1 and APL termini, further increasing the complexity of interactions between OA innervation and the KC/APL negative feedback look.

GRASP analyses also suggested that PNs are postsynaptic to the sVUM1 neurons. Indeed, we found that the alpha-1-adrenergic receptor homolog Oamb (based on classification by Roeder et al. (2003) and Verlinden et al. (2010)) is expressed by PNs and an exon-trap Oamb::eGFP fusion localized to PN presynaptic terminals. Oamb (also known as Dmoa1A or

CG3856), signals through Gαq and release of Ca^{2+} from intracellular stores (Balfanz et al., 2005; Morita et al, 2006). Consistent with our observations in *Drosophila*, the honeybee Oamb ortholog AmOA1 is also found in the calyx (Sinakevitch et al., 2011).

An increase in Ca^{2+} in PN presynaptic terminals by action of OA on Oamb receptors, could potentially enhance acetylcholine release from PN terminals onto KC dendrites, and therefore serve as a gating mechanism (Hurley et al. 2004), increasing signal to noise ratio, and allowing the detection of weak signals under conditions that promote OA release. Enhanced response of peripheral sensory receptors by OA has been previously reported: enhancement to mechanical stimuli in proprioceptors of the hindleg by direct stimulation of octopaminergic DUM neurons was reported (Bräunig and Eder, 1998). A similar mechanism of increase in sensitivity to mechanical stimuli mediated by octopamine action on OAMB receptors in sensory efferents innervating mechanosensory receptors in the spider have been reported (Widmer et al., 2005).

We also found that the sVUM1 neurons make significant contacts with Odd neurons, Although we do not currently understand the physiological significance of these contacts, the wide arborization of the Odd neurons in the calyx [may allow them to monitor non-specific sensory responses in the calyx, and OA innervation would mean that this could potentially be modulated.

Clearly OA has potentially wide actions on different cell types in the calyx, and a more complete analysis of the receptors localized on its target neurons is necessary to unravel its global effect on MB calyx activity. While we did not detect convincing signals with EGFP fusions to OctBeta receptors, we do not know whether these fusions are functional.

Odor discrimination behavior

A role for OA in reward signaling has been established in honeybees and flies. Work on honeybees suggests the VUMmx1 neuron as a reward neuron in associative learning in honeybees; honeybee VUMmx1 could replace sugar reinforcement signal in an appetitive associative learning paradigm (Hammer 1993), and injection of OA into the MB calyx induced memory consolidation (Hammer and Menzel, 1998). However results in *Drosophila* are less straightforward to interpret, Stimulation of neurons including OA-VUMa2, the adult equivalent of larval VUMmx1 (Busch et al. 2009), using *NP7088-GAL4* and *dTrpA1*, did not induce appetitive learning (Burke et al. 2012). On the other hand, learning was induced by stimulation of *Tdc2-GAL4*, and OAMB receptor expressed in PAM dopamine neurons that target the MB lobes is required for OA-dependent appetitive associative learning. Furthermore, Oamb is

required in KCs for appetitive learning (Kim et al., 2013); while this may be at first sight contradictory with our finding that Oamb::EGFP is localized to PNs and not KCs in the calyx, Oamb is also localized in MB lobes, and could be required there for appetitive learning. Taken together, these targeted expression experiments suggest an indirect function of OA in sugar reward learning by acting on dopaminergic neurons that innervate the MB lobes, but do not rule out effects via the calyx that could contribute to appetitive learning under some circumstances. Our results support a role of OA in sensory processing and discriminaton, rather than learning, because the ability to discriminate dissimilar odors, and thus underlying learning ability, was not affected.

To target activation of CsChrimson more specifically to the sVUM1 neurons, we used a pair of intersectional lines, whose overlap labels two mandibular sVUM neurons, two maxillary sVUM neurons, and one labial sVUM neuron (which does not project to the brain, Selcho et al., 2014), This pattern includes sVUMmx1 and VUMmd1, both of which innervate the AL and calyx. The second sVUM in the mandibular and maxillary neuromeres could not be identified due to merging of axonal pathways, but is likely to be either sVUM2 or sVUM3, which Selcho et al. (2014) have described in each of these neuromeres, neither of which innervate the AL nor the MBs.

Perspectives

Mammalian olfactory neuropiles are densely innervated by noradrenergic input, similar to the dense OA innervation of AL and calyx by sVUM1 neurons in insects. The innervation of sVUM1 neurons throughout the calyx, and their potential synaptic connections to PNs, APL, and odd-like neurons, suggest that OA input to the calyx, induces a network level switch both via input afferents on the overall activity of the calyx, and by interacting with the KC/APL feedback loop, and thus also affecting the output activity from the calyx – not only through KCs but also potentially via the Odd neurons. At least in PNs, OAMB, the alpha-1-adrenergic receptor ortholog, could act as a gate control by modulating the release of PN afferent neurotransmitter. Enhancement of afferent PN transmitter release would increase sensory input to KCs, with predicted consequences of increase in sensitivity versus decrease in discrimination. Increase in sensitivity would evoke a stronger KC output in response to weaker signals, at the expense of odor discrimination, which could be crucial for the detection of certain odors depending on circumstance.

Acknowledgements:

We thank T. Awasaki, S Certel, K. Ito, M Landgraf, T. Lee, C.H.-Lee, B Pfeiffer, M. Ramaswami, K. Scott, J Truman, and the Bloomington Drosophila Stock Center (BDSC) for numerous fly stocks, and the Developmental Studies Hybridoma Bank (DSHB), University of Iowa, for antibodies. We thank S Assadullah, Dixy Shah for help in generating IT.GAL4 insertions, Tom Bland for helping set up the larval behavior assay, and M Morgan for help in building optogenetic illumination apparatus.

JYHW was supported by a Medical Research Council studentship and MM was supported by a UK Genetics Society “Genes and Development” summer scholarship and an award from the Bedford Fund, King’s College Cambridge. This work was supported by BBSRC Grants BB/I022651/1 and BB/N007948/1 and an Isaac Newton Trust award to LMM-N and CJO’K.

References

1. Altschul, S.F., Gish, W., Miller, W., Myers, E.W., and Lipman, D.J. (1990). Basic local alignment search tool. J. Mol. Biol. *215*, 403–410.
2. Balfanz, S., Strünker, T., Frings, S., and Baumann, A. (2005). A family of octopamine receptors that specifically induce cyclic AMP production or Ca2+ release in Drosophila melanogaster. J. Neurochem. *93*, 440–451.
3. Berridge, C.W., and Waterhouse, B.D. (2003). The locus coeruleus-noradrenergic system: modulation of behavioral state and state-dependent cognitive processes. Brain Res. Revs. *42*, 33-84.
4. Bouret, S., and Sara, S.J. (2002) Locus coeruleus activation modulates firing rate and temporal organization of odour-induced single-cell responses in rat piriform cortex. Eur. J. Neurosci. *16*, 2371-2382.
5. Bräunig, P. (1991). Suboesophageal DUM neurones innervate the principal neuropiles of the locust brain. Philos Trans R Soc Lond Biol *332*, 221–240.
6. Bräunig, P., and Eder, M. (1998). Locust dorsal unpaired median (DUM) neurons directly innervate and modulate hindleg proprioreceptors. J. Exp. Biol. *201*, 3333-3338.
7. Burke, C.J., Huetteroth, W., Owald, D., Perisse, E., Krashes, M.J., Das, G., Gohl, D., Silies, M., Certel, S., and Waddell, S. (2012). Layered reward signalling through octopamine and dopamine in Drosophila. Nature *492*, 433–437.
8. Busch, S., Selcho, M., Ito, K., and Tanimoto, H. (2009). A map of octopaminergic neurons in the *Drosophila* brain. J. Comp. Neurol., *513*, 643-667.
9. Ciombor, K.J., Ennis, M, and Shipley, M.T. (1999). Norepinephrine increases rat mitral cell excitatory responses to weak olfactory nerve input via alpha-1 receptors in vitro. Neurosci. *90*, 595-606.
10. Cole, S.H., Carney, G.E., McClung, C.A., Willard, S.S., Taylor, B.J., and Hirsh, J. (2005. Two functional but noncomplementing *Drosophila* tyrosine decarboxylase genes. J. Biol. Chem. *280*, 14948-14955.
11. Deady, L.D., and Sun, J. (2015). A Follicle Rupture Assay Reveals an Essential Role for Follicular Adrenergic Signaling in Drosophila Ovulation. PLoS Genet. *11*, 1–21.
12. de Vries, S.E., Clandinin, T. (2013). Optogenetic Stimulation of Escape Behavior in *Drosophila melanogaster*. *J. Vis. Exp.* (71), e50192.
13. Doucette, W., Milder, J., and Restrepo, D. (2007). Adrenergic modulation of olfactory bulb circuitry affects odor discrimination. Learn Mem *14*, 539-547.
14. Doucette, W., Gire, D.H., Whitesell, J., Carmean, V., Lucero, M.T., and Restrepo, D. (2011).

Associative cortex features in the first olfactory brain relay station. Neuron *69*, 1176-1187.

15. Eichler, K., Li, F., Litwin-Kumar, A., Park, Y., Andrade, I., Schneider-Mizell, C.M., Saumweber, T., Huser, A., Eschbach, C., Gerber, B., Fetter, R.D., Truman, J.W., Priebe, C.E., Abbott, L.F., Thum, A.S., Zlatic, M., and Cardona, A. (2017). The complete connectome of a learning and memory centre in an insect brain. Nature 548, 175-182.
16. Estes, P.S., Ho, G.L.Y., Narayanan, R., and Ramaswami, M. (2000). Synaptic localization and restricted diffusion of a *Drosophila* neuronal synaptobrevin - green fluorescent protein chimera in vivo. J. Neurogenet. *13*, 233-255.
17. Gohl, D.M., Silies, M.A., Gao, X.J., Bhalerao, S., Luongo, F.J., Lin, C.-C., Potter, C.J., and Clandinin, T.R. (2011). A versatile in vivo system for directed dissection of gene expression patterns. Nat. Meths. *8*, 231-241.
18. Goosey, M.W., and Candy, D.J. (1980). Effects of D- and L-octopamine and of pharmacological agents on the metabolism of locust flight muscle. Biochem. Soc. Trans. *8*, 532-533
19. Gordon, M. D., and Scott, K. (2009). Motor control in a *Drosophila* taste circuit. Neuron 61, 373-384.
20. Hammer, M. (1993). An identified neuron mediates the unconditioned stimulus in associative olfactory learning in honeybees. Nature *366*, 59-63.
21. Hammer, M. and Menzel, R. (1998). Multiple sites of associative odor learning as revealed by local brain injections of octopamine in honeybees. Learn. Mem. *5*, 146-156.
22. Han, K. A, Millar, N.S., and Davis, R.L. (1998). A novel octopamine receptor with preferential expression in *Drosophila* mushroom bodies. J. Neurosci. *18*, 3650–3658.
23. Han, C., Jan, L.Y., and Jan, Y.-N. (2011). Enhancer-driven membrane markers for analysis of nonautonomous mechanisms reveal neuron-glia interactions in *Drosophila*. Proc. Natl. Acad. Sci. USA *108*, 9673-9678.
24. Hurley, L.M., Devilbiss, D.M., and Waterhouse, B.D. (2004). A matter of focus: monoaminergic modulation of stimulus coding in mammalian sensory networks. Curr. Opin. Neurobiol. *14*, 488-495.
25. Jenett, A., Rubin, G.M., Ngo, T.-T.B., Shepherd, D., Murphy, C., Dionne, H., Pfeiffer, B.D., Cavallaro, A., Hall, D., Jeter, J., et al. (2012). A GAL4-driver line resource for *Drosophila* neurobiology. Cell Reps. *2*, 991-1001.
26. Karuppudurrai, T., Lin, T.-Y., Ting, C.-Y., Pursley, R., Melnattur, K. V., Diao, F., White, B. H., Macpherson, L. J., Gallio, M., Pohida, T., and Lee, C.-H. (2014). A hard-wired glutamatergic circuit pools and relays UV signals to mediate spectral preference in Drosophila. Neuron 81, 603-615.

27. Kim, Y.-C., Lee, H.-G., Lim, J., and Han, K.-A. (2013). Appetitive learning requires the alpha1-like octopamine receptor OAMB in the Drosophila mushroom body neurons. J. Neurosci. *33*, 1672–1677.
28. Klapoetke, N. C., Mutata, Y., Kim, S.S., Pulver, S.R., Birdsey-Benson, A., Cho, Y.K., Morimoto, T.K., Chuong, A.S., Carpenter, E.J., Tian, Z., Wang, J., Xie, Y., Yan, Z., Zhang, Y., Chow, B.Y., Surek, B., Melkonian, M., Jayaraman, V., Constantine-Paton, M., Wong, G.K.-S., and Boyden, E.S. (2014). Independent optical excitation of distinct neural populations. Nat. Meths. 11, 338-351.
29. Lee, T., and Luo, L. (1999). Mosaic analysis with a repressible cell marker for studies of gene function in neuronal morphogenesis. Neuron *22*, 451-461.
30. Lin, A.C., Bygrave, A.M., de Calignon, A., Lee, T., and Miesenböck, G. (2014). Sparse, decorrelated odor coding in the mushroom body enhances learned odor discrimination. Nat. Neurosci. *17*, 559–568.
31. Maqueira, B., Chatwin, H., and Evans, P.D. (2005). Identification and characterization of a novel family of Drosophila beta-adrenergic-like octopamine G-protein coupled receptors. J. Neurochem. *94*, 547–560.
32. Masuda-Nakagawa, L.M., Tanaka, N.K., and O'Kane, C.J. (2005). Stereotypic and random patterns of connectivity in the larval mushroom body calyx of Drosophila. Proc. Natl. Acad. Sci. USA. *102*, 19027–19032.
33. Masuda-Nakagawa, L.M., Gendre, N., O'Kane, C.J., and Stocker, R.F. (2009). Localized olfactory representation in mushroom bodies of Drosophila larvae. Proc. Natl. Acad. Sci. USA. *106*, 10314–10319.
34. Masuda-Nakagawa, L.M., Ito, K., Awasaki, T., and O'Kane, C.J. (2014). A single GABAergic neuron mediates feedback of odor-evoked signals in the mushroom body of larval Drosophila. Front. Neural Circuits *8*, 35.
35. Morita, M., Susuki, J., Amino, H., Yoshiki, F., Moizumi, S., and Kudo, Y. (2006). Use of the exogenous Drosophila octopamine receptor gene to study Gq-coupled receptor-mediated responses in mammalian neurons. Neuroscience *137*, 545–553.
36. Nagarkar-Jaiswal, S., Lee, P., Campbell, M.E., Chen, K., Anguiano-zarate, S., Gutierrez, M.C., Busby, T., Lin, W., He, Y., Schulze, K.L., et al. (2015). A library of MiMICs allows tagging of genes and reversible spatial and temporal knockdown of proteins in *Drosophila*. eLife *4*, e05338.
37. Nern, A., Pfeiffer, B.D., and Rubin, G.M. (2015). Optimized tools for multicolor stochastic labeling reveal diverse stereotyped cell arrangements in the fly visual system. Proc Natl. Acad. Sci. USA. *112*, E2967-E2076.

38. Orchard, I., Loughton, B.G., and Webb, R.A. (1981). Octopamine and short-term hyperlipaemia in the locust. Gen. Compar. Endocrinol. *45*, 175-180.
39. Perez-Orive J., Mazor, O., Turner, G.C., Cassenaer, S., Wilson, R.I., and Laurent, G. (2002). Oscillations and sparsening of odor representations in the mushroom body. Science *297*, 359-365.
40. Pfeiffer, B.D., Ngo, T.-T.B., Hibbard, K.L., Murphy, C., Jenett, A., Truman, J.W., and Rubin, G.M. (2010). Refinement of tools for targeted gene expression in Drosophila. Genetics *186*, 735–755.
41. Pitman, J.L., Huetteroth, W., Burke, C.J., Krashes, M.J., Lai, S.-L., Lee, T., and Waddell, S. (2011). A pair of inhibitory neurons are required to sustain labile memory in the *Drosophila* mushroom body. Curr. Biol. *21*, 855-861.
42. Roeder, T., Seifert, M., Kähler, C., and Gewecke, M. (2003). Tyramine and octopamine: antagonistic modulators of behavior and metabolism. Arch. Insect. Biochem. Physiol. *54*, 1-13.
43. Sara, S.J. (2009). The locus coerulus and noradrenergic modulation of cognition. Nat. Revs. Neurosci. *10*, 211-223.
44. Sara, S.J. and Bouret, S (2012). Orienting and reorienting: the Locus Coeruleus mediates cognition through arousal. Neuron 76, 130-141.
45. Schroll, C., Riemensperger, T., Bucher, D., Ehmer, J. Völler, T., Erbguth, K., Gerber, B., Hendel, T., Nagel, G., Buchner, E., and Fiala, A. (2006). Light-induced activation of distinct modulatory neurons triggers appetitive or aversive learning in *Drosophila* larvae. Curr. Biol. *16*, 1741-1747.
46. Schröter, U., Malun, D., and Menzel, R. (2007). Innervation pattern of suboesophageal ventral unpaired median neurones in the honeybee brain. Cell Tissue Res. *327*, 647-667.
47. Schwaerzel, M., Monastirioti, M., Scholz, H., Friggi-Grelin, F., Birman, S., and Heisenberg, M. (2003). Dopamine and octopamine differentiate between aversive and appetitive olfactory memories in *Drosophila*. J Neurosci. *23*, 10495-10502.
48. Selcho, M., Pauls, D., Huser, A., Stocker, R.F., and Thum, A.S. (2014). Characterization of the octopaminergic and tyraminergic neurons in the central brain of Drosophila larvae. J. Comp. Neurol. *522*, 3485–3500.
49. Sinakevitch, I., Mustard, J.A., and Smith, B.H. (2011). Distribution of the octopamine receptor AmOA1 in the honey bee brain. PLoS One *6*, e14536.
50. Slater, G., Levy, P., Chan, K.L.A., and Larsen, C. (2015). A Central Neural Pathway Controlling Odor Tracking in *Drosophila*. J. Neurosci. *35*, 1831–1848.
51. Sonnhammer, E.L., von Heijne, G., and Krogh, A. (1998). A hidden Markov model for

predicting transmembrane helices in protein sequences. Proc. ISMB *6*, 175–182.

52. Stern, M. (1999). Octopamine in the locust brain: cellular distribution and functional significance in an arousal mechanism. Microsc. Res. Tech. *45*, 135-141.
53. Stopfer, M., Bhagavan, S. Smith, B.H., and Laurent, G. (1997). Impaired odour discrimination on desynchronization of odour-encoding neural assemblies. Nature 390, 70-74.
54. Tanaka, N.K., Awasaki, T., Shimada, T., and Ito, K. (2004). Integration of Chemosensory Pathways in the Drosophila Second-Order Olfactory Centers. Curr. Biol. *14*, 449–457.
55. Venken, K.J.T., Schulze, K.L., Haelterman, N. a, Pan, H., He, Y., Evans-Holm, M., Carlson, J.W., Levis, R.W., Spradling, A.C., Hoskins, R. a, et al. (2011). MiMIC: a highly versatile transposon insertion resource for engineering Drosophila melanogaster genes. Nat. Methods *8*, 737–743.
56. Verlinden, H., Vleugels, R., Marchal, E., Badisco, L., Pflüger, H.-J., Blenau, W., and Vanden Broeck, J. (2010). The role of octopamine in locusts and other arthropods. J. Insect Physiol. *56*, 854-867.
57. Widmer, A., Höger, U., Meisner, S., French, A.S. and Torkkeli, P.H. (2005). Spider peripheral mechanosensory neurons are directly innervated and modulated by octopaminergic efferents. J. Neurosci. *25*, 1588-1598.

.

Figure Legends

Figure 1. Behavioral discrimination assay and optogenetics.

Larvae are conditioned for three cycles of: a container with one odor (in this case ethyl acetate, EA) and a container lacking odor (C) on a agar sucrose plate (red), followed by a container with a different odor (in this case pentyl acetate, PA) and a container lacking odor, on an agar plate (light gray). Larvae are then tested by being placed on an oblong area in the middle of an agar plate, with a choice of EA or PA, and a black background to provide contrast for counting larvae. A different group of larvae are conditioned and tested with reciprocal odor pairing. Control experiments (top row) are carried out in dim blue light. Optogenetic activation of CsChrimson is accomplished by amber light during the conditioning phases.

Figure 2. MutiColor FlpOut of *Tdc2-GAL4*-expressing neurons labels two calyx-innervating neurons.

Single cell clones of the larval progeny of *Tdc2-GAL4* crossed to *pBPhsFlp2::PEST(attP3); HA_V5_FLAG_OLLAS,* were generated by heat shock expression of FLP. **A.** A 3D stereo projection of a neuron labeled in magenta (V5 tag) and another labeled in green (HA tag), both ramifying throughout the calyx. Arrowheads show the axons of the two neurons. **B**. Cell bodies in the SEZ region of the same larva. In the mandibular (top) neuromere, two cell bodies labeled in magenta can be identifed labeled by antibody to V5 (arrowheads). One of these is the sVUM1md neuron. In the maxillary (bottom) neuromere, a single cell body is only green, identified by anti-HA (arrowhead). Scale bars: 10 µm in A, 15 µm in B.

Figure 3. Polarity of calyx innervation by *Tdc2-GAL4*-expressing neurons.

A. 3D stereo projection of a 3rd instar larval calyx expressing nSyb::GFP and CD4::Tom using *Tdc2-GAL4*. Two axonal tracts (arrowheads) enter the calyx and ramify throughout the calyx (CD4::tdTom), while processes show nSyb::GFP localization in boutons (green). Notice boutons at the borders of glomeruli (e.g. arrow) and core of the calyx (e.g. asterisk). **B.** Confocal section through the calyx of a larva expressing DenMark::mCherry and Syt::GFP using *Tdc2-GAL4*. **C.** Confocal section of the brain of a larva expressing DenMark::mCherry and Syt::GFP using *Tdc2-GAL4*. Arrowheads indicate the primary processes of *Tdc2-GAL4*-expressing neurons in md (top arrowhead) and mx (bottom arrowhead) neuromeres. **A**, **B**: Anterior is to the bottom, medial to the right. Right brain orientation is shown. **C**: Ventral view, anterior is to top.

Figure 4. GRASP shows calyx contacts of sVUM1 termini with PNs, larval APL, and *odd*-like neurons, but not KCs.

All panels are confocal sections, showing GRASP signals as GFP fluorescence, obtained using the sVUM1 lines *Tdc2-LexA* or *Tdc2-GAL4*, and *GAL4* or *LexA* lines expressed in different calyx neurons, driving GRASP constructs *UAS-CD4::spGFP1-10* and *LexAop-CD4::spGFP11* sVUM1.

A. GRASP signal between sVUM1 neurons and other calyx neurons is detected as GFP fluorescence, using the *GAL4* and *LexA* lines shown.

B-C. GRASP signal between sVUM1 neurons and other calyx neurons, driven using the *GAL4* and *LexA* lines shown, is detected using anti-GFP. Examples of GRASP signal are highlighted with arrowheads; areas inside broken line are shown at higher zoom. sVUM1 termini are labeled using anti-OA; calyx glomeruli are labeled using anti-Dlg.

B. GRASP signal between sVUM1 termini and PNs, localised mainly around glomeruli. OA signals without GRASP are localised to the calyx core. GRASP signal overlaps partially with sVUM1 termini labelled with OA (inset). GFP signals devoid of OA are presumptive axonal tracts and not synaptic.

C. GRASP signal between sVUM1 termini (OA, top row) and the GABAergic larval APL neuron. GRASP signals are localised around glomeruli, or in the core of the calyx. Lower panels show GRASP signals overlapping partially with large GABA boutons.

D. Confocal sections of a 3rd instar larval calyx expressing *mCD8::GFP* using *Tdc2-Gal4* and labeled with anti-GABA and anti-Dlg. Top is dorsal section of calyx, bottom is a ventral section of the same calyx. Arrowheads indicate GABA boutons apposed to or overlapping with *Tdc2* neuron terminals. Arrows indicate the two axonal tracts of *Tdc2* neurons innervating the calyx.

E. GRASP signals between sVUM1 termini and Odd neurons. Examples of GRASP signal are highlighted with arrowheads; areas inside broken line, and a GRASP signal next to an asterisk, are shown at higher zoom.

F. No detectable GRASP signals between sVUM1 termini and KC dendrites.

Figure 5. Single cell GRASP of sVUM1 neurons in the calyx.

A. Identification of sVUM1 neurons based on SEZ anatomical landmarks. Larval brains carrying *Tdc2-LexA*, *GMR34A11-GAL4*, *LexAop-FLP*, *tub>GAL80>* and *UAS-Chrimson::Venus*, showing Venus expression in a subset of the cells expressing both *Tdc2-LexA* and *GMR34A11-GAL4*. sVUM1md neurons (Md) are in a small anterior medial Dlg-negative gap, with characteristic Dlg-negative bilaterally symmetrical gaps (asterisks) nearby.

sVUM1mx neurons (Mx) are localized in a large medial Dlg-negative gap (arrowhead) that lies just anterior to a commissural DLG pathway (arrowheads). sVUMlb neurons (Lb) are localized posteriorly to this commissural pathway. Scale bar 24 µm.

B-E. Single-cell GRASP was induced between sVUM1 neurons expressing *Tdc2-LexA*, and potential calyx partner neurons that expressed different *GAL4* lines. sVUM1 neurons were individually labeled by heat-shock-induced FlipOut of larvae carrying *P{hsFLP}12, Tdc2-LexA, GAL4*, *LexAOp2-IVS>stop>spGFP11::CD4::HA-T2A-Brp::mCherry (attP2), UAS-spGFP1-10::CD4, UAS- HRP::CD2*.

B. Single cell clone generation showing expression of Brp::mCherry in subsets of *Tdc2-LexA*-expressing neurons; each row shows a separate clone. Left image pairs are stereo views of reconstructions showing the entire trajectory of labelled neurons; right images are single confocal sections through the SEZ of the same larvae, showing the primary process of each labelled sVUM1 (arrows) and the anatomical landmarks shown in **A**. First row, sVUMmd1 and sVUMmx1. Second row, sVUM md1. Third row, sVUM mx1. Scale bar is 45 µm in 3D images (Left), 30 µm in SEZ sections (Right). *OK263-GAL4* (top and middle rows) or *NP2631-GAL4* (bottom row) are also present, but do not contribute to any of the staining shown.

C-E. Single-cell GRASP between sVUM1 neurons expressing *Tdc2-LexA*, and larval APL expressing (**C**) *NP2631-GAL4*, (**D**) Odd neurons expressing *OK263-GAL4* or (**E**) KCs expressing *H275-IT.GAL4*. Left panels: calyx of larval brain labelled with anti-DsRed to visualise presynaptic sites, anti-Dlg to label neuropile, and anti-GFP to visualise GRASP signals. Arrows indicate GRASP signals. Scale bar: 10 µm. Right panel: region of same brain labelled with anti-Dlg to visualise neuropile, and anti-DsRed to visualize the VUM neurons. Top rows show sVUMmd1 (Md), bottom rows show sVUMmx1 (Mx). Arrows indicate the primary process of each sVUM1 neuron.

Figure 6. Oamb-GFP localization in PN presynaptic termini. **A.** Calyces of a larva carrying *Oamb::EFGP*, *NP225-GAL4* and *UAS-RFP* labelled with antibodies to GFP, DsRed and Dlg. Oamb::EGFP localizes to PN terminals in all glomeruli labelled in line *NP225-GAL4*, and additionally to a few glomeruli innervated by non-olfactory PNs, not labelled by line *NP225-GAL4* (arrowheads). A few glomeruli show neither *NP225-GAL4* nor Oamb::EFGP expression (asterisks). **B.** Oamb::EGFP does not overlap with APL termini labelled by anti-GABA (top row) or with projections of the APL labelled using *NP732-GAL4* (bottom row). **C.** Oamb::EGFP does not show substantial overlap with Odd neuron dendrites labelled using *OK263-GAL4*. Scale bar, 10 µm.

Figure 7. Activation of a small subset of OA neurons including the sVUM1 neurons disrupts odor discrimination but not learning. A. A pair of stereo images showing CsChrimson::mVenus expressed in a small subset of OA neurons, using the genotype shown in Fig. 5A. The mandibular, maxillary and labial (Md, Mx, Lb) clusters are shown, which include the sVUMmd1 and sVUMmx1 neurons, which innervate the calyx. Scale bar, 40 μm. **B.** Activation of the neurons labelled in A by CsChrimson occurs in the presence of retinal and amber light, and abolishes odor choice learning using similar odor pairs, compared to controls exposed to blue light, lacking retinal, or tested with dissimilar odor pairs. No effect of CsChrimson activation is seen on learning using dissimilar odor pairs. Planned statistical comparisons shown are t-tests (***, $P < 0.0001$, NS, $P > 0.6$). An ANOVA test across all data from two experimenters showed no significant effect of experimenter either alone, or as interactions with other factors ($P>0.2$). ANOVA tests also showed no significant effect of odor alone ($P>0.03$, not significant with multiple testing), retinal alone ($P>0.4$), or light alone ($P>0.2$), when comparisons that would have included the retinal, amber, similar combination with the strong effect were excluded.

Fig 1

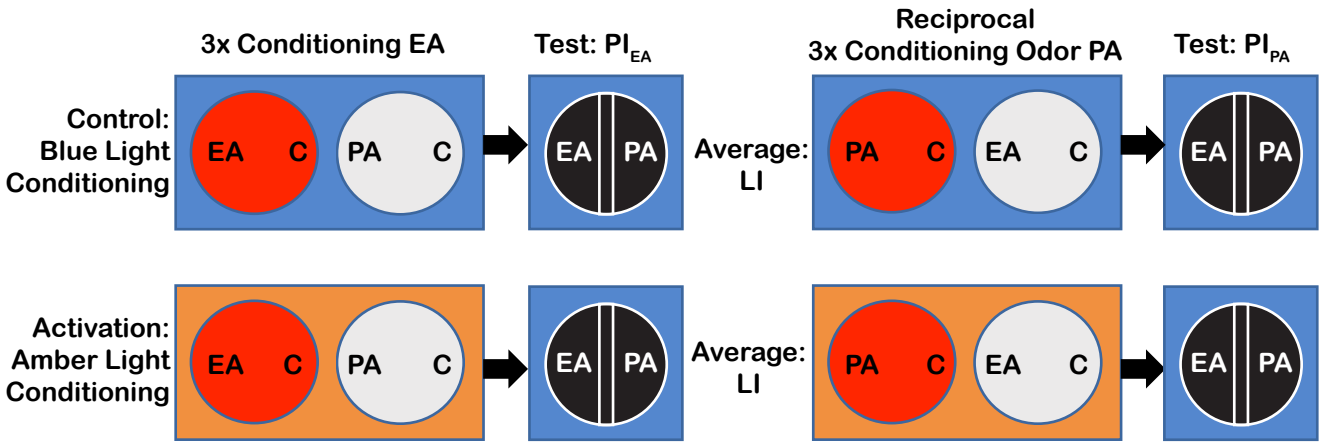
3x Conditioning EA
Test: PI_{EA}
Reciprocal
3x Conditioning Odor PA
Test: PI_{PA}
Control:
Blue Light
Conditioning
EA
C
PA
C
EA
PA
Average:
LI
PA
C
EA
C
EA
PA
Activation:
Amber Light
Conditioning
EA
C
PA
C
EA
PA
Average:
LI
PA
C
EA
C
EA
PA

Fig 2

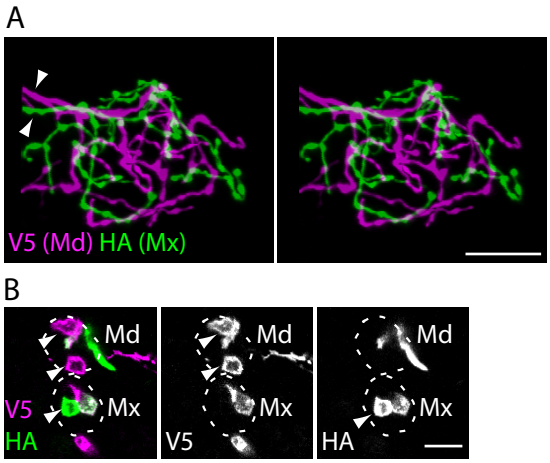

Fig 3

A

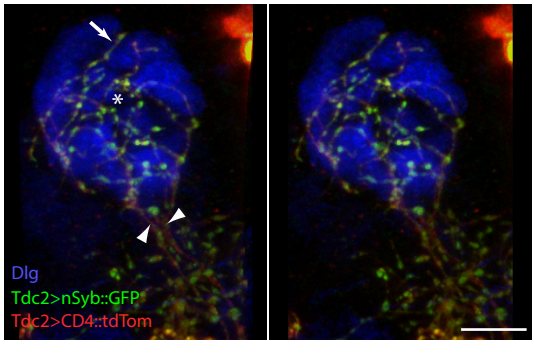
Dlg
Tdc2>nSyb::GFP
Tdc2>CD4::tdTom

B

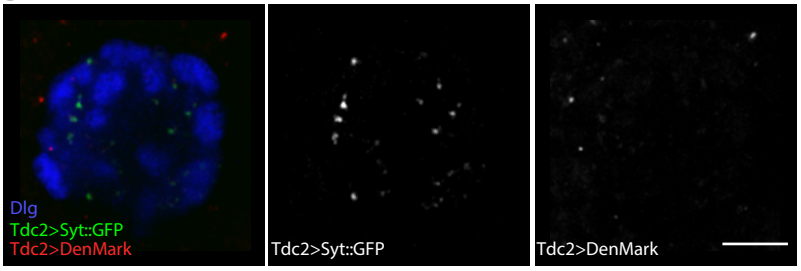
Dlg
Tdc2>Syt::GFP
Tdc2>DenMark
Tdc2>Syt::GFP
Tdc2>DenMark

C

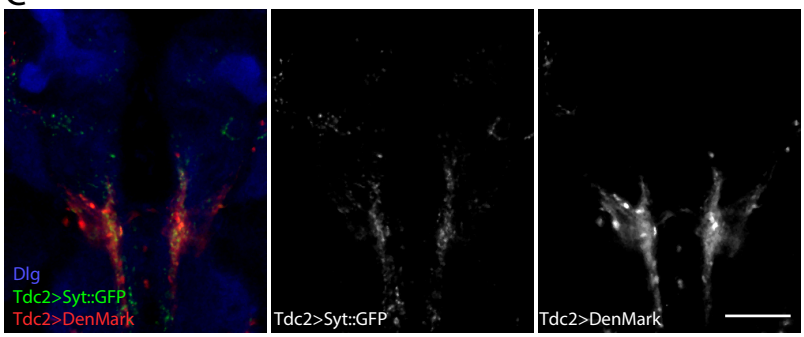
Dlg
Tdc2>Syt::GFP
Tdc2>DenMark
Tdc2>Syt::GFP
Tdc2>DenMark

Figure 4

A

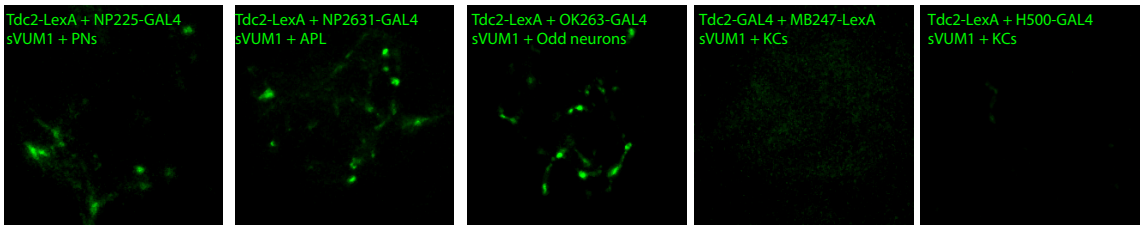

B

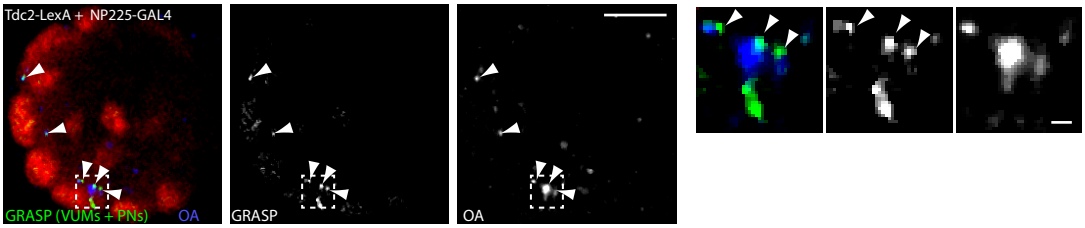

C

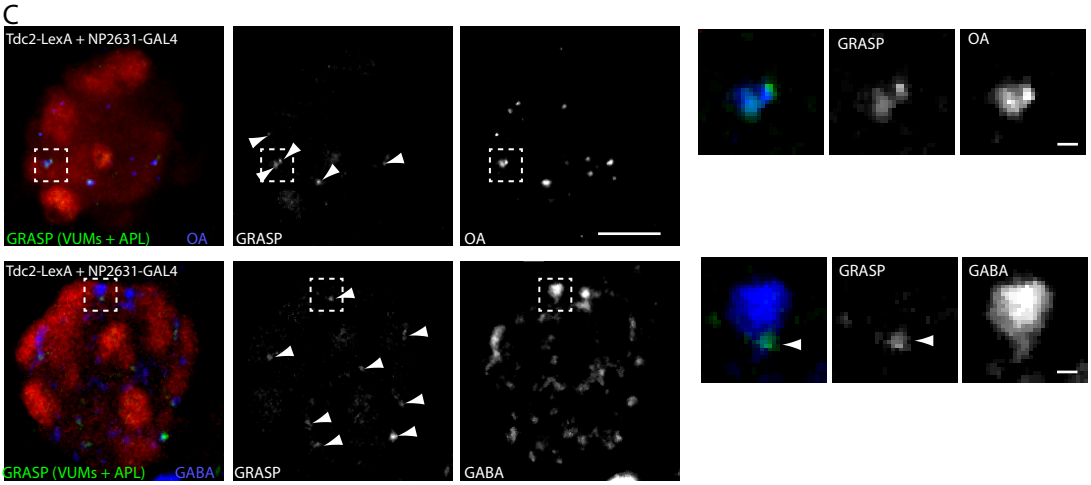

D

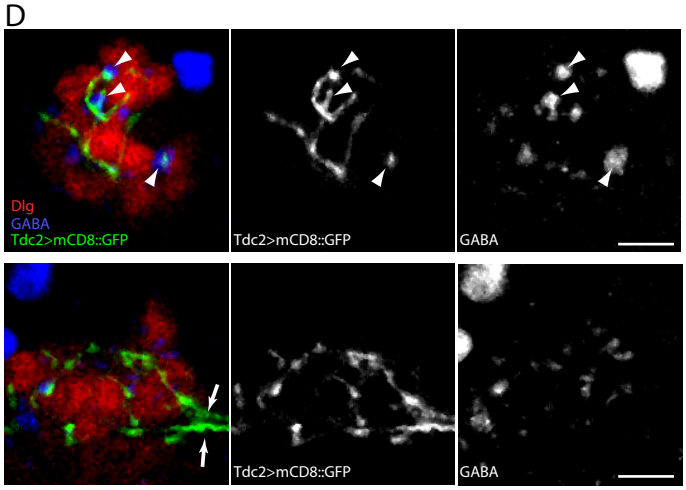

E

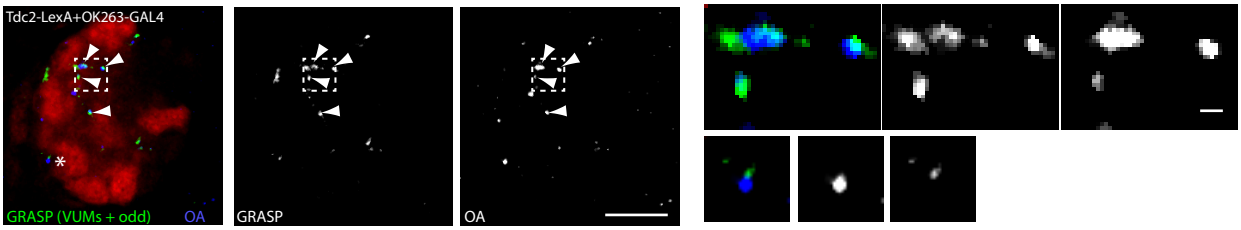

F

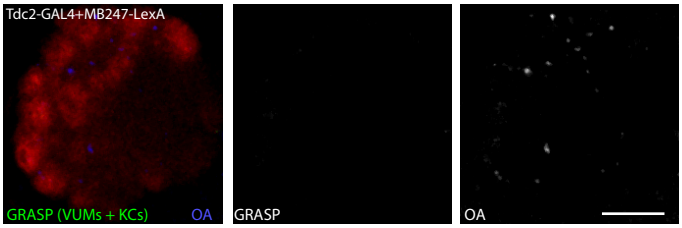

Figure 5

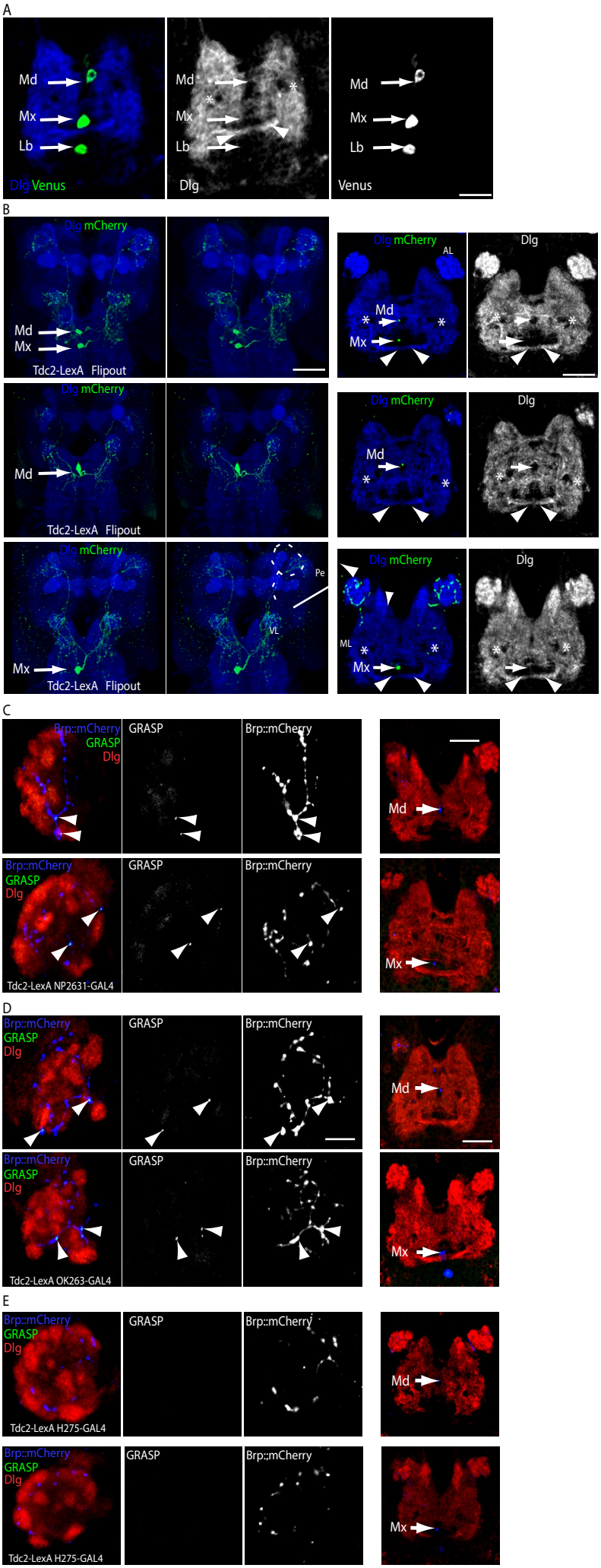
A
Md
Mx
Lb
Dlg Venus
Md
Mx
Lb
Dlg
Md
Mx
Lb
Venus
B
Dlg mCherry
Md
Mx
Tdc2-LexA Flipout
Dlg mCherry
AL
Md
Mx
Dlg
Dlg mCherry
Md
Tdc2-LexA Flipout
Dlg mCherry
Md
Dlg
Dlg mCherry
Pe
VL
Mx
Tdc2-LexA Flipout
Dlg mCherry
ML
Mx
Dlg
C
Brp::mCherry
GRASP
Dlg
GRASP
Brp::mCherry
Md
Brp::mCherry
GRASP
Dlg
GRASP
Brp::mCherry
Mx
Tdc2-LexA NP2631-GAL4
D
Brp::mCherry
GRASP
Dlg
GRASP
Brp::mCherry
Md
Brp::mCherry
GRASP
Dlg
GRASP
Brp::mCherry
Mx
Tdc2-LexA OK263-GAL4
E
Brp::mCherry
GRASP
Dlg
GRASP
Brp::mCherry
Md
Tdc2-LexA H275-GAL4
Brp::mCherry
GRASP
Dlg
GRASP
Brp::mCherry
Mx
Tdc2-LexA H275-GAL4

Figure 6

A

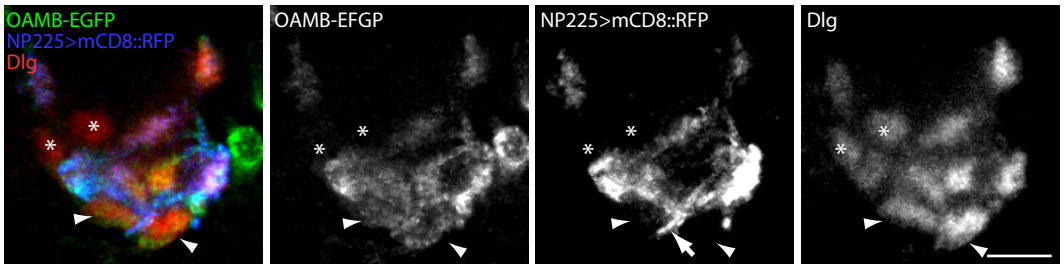
OAMB-EGFP
NP225>mCD8::RFP
Dlg
OAMB-EFGP
NP225>mCD8::RFP
Dlg

B

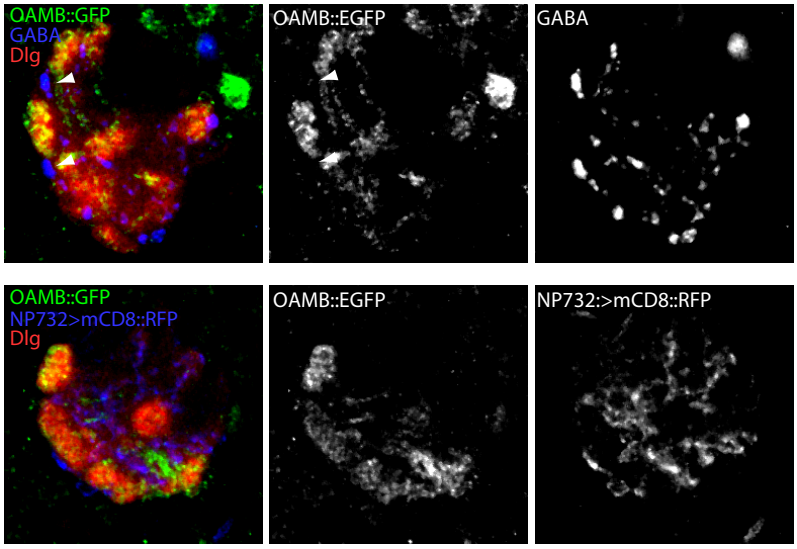
OAMB::GFP
GABA
Dlg
OAMB::EGFP
GABA
OAMB::GFP
NP732>mCD8::RFP
Dlg
OAMB::EGFP
NP732:>mCD8::RFP

C

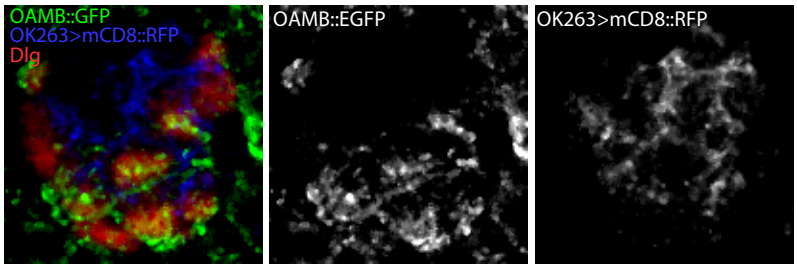
OAMB::GFP
OK263>mCD8::RFP
Dlg
OAMB::EGFP
OK263>mCD8::RFP

Figure 7

A

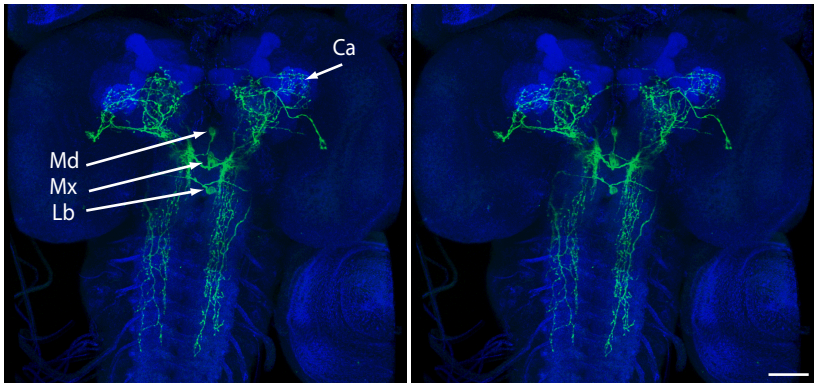
Ca
Md
Mx
Lb

B

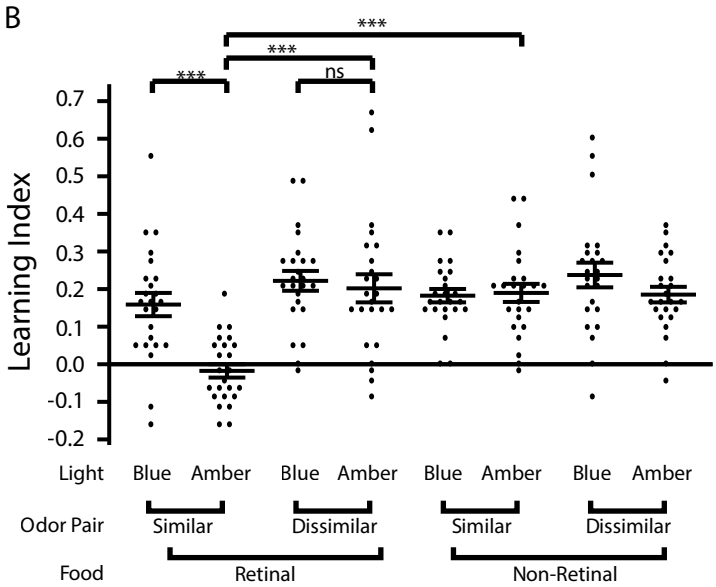
***
***
***
ns
Learning Index
0.7
0.6
0.5
0.4
0.3
0.2
0.1
0.0
-0.1
-0.2
Light
Blue
Amber
Blue
Amber
Blue
Amber
Blue
Amber
Odor Pair
Similar
Dissimilar
Similar
Dissimilar
Food
Retinal
Non-Retinal

Table 1. *Drosophila* stocks used.

Genotype	Source	Reference	Use
NP2631-GAL4	T Awasaki, K Ito	Masuda-Nakagawa et al., 2014	APL neuron line
NP732-GAL4	T Awasaki, K Ito	Masuda-Nakagawa et al., 2014	APL neuron line
NP225-GAL4	T Awasaki, K Ito	Masuda-Nakagawa et al. 2005	PN line
OK263-GAL4	COK, LMN	Unpublished	OK263 neuron line
GMR34A11-GAL4	BDSC 52755	Jenett et al., 2012	sVUM1 neuron line
H275-IT.GAL4	This work	Gohl et al., 2011	*KC line*
H500-IT.GAL4	This work	Gohl et al., 2011	*KC line*
Tdc2-GAL4	BDSC 9313	Cole et al., 2005	*OA neuron line*
Tdc2-LexA	S Certel, S Waddell	Burke et al., 2012	*OA neuron line*
MB247-LexA	T Lee	Pitman et al., 2011	KC line
GMR34A11-LexA	BDSC 52755	Jenett et al, 2012	sVUM1 neuron line
UAS-mCD8::GFP	BDSC 5130	Lee and Luo, 1999	mCD8::GFP reporter
10XUAS-IVS-mCD8::RFP (attP40) (II)	BDSC 32219	Pfeiffer et al., 2010	mCD8::RFP reporter
13XLexAOp-mCD8::GFP	BDSC 32203	Pfeiffer et al., 2010	mCD8::GFP reporter
UAS-CD4::tdTomato	BDSC 35841	Han et al., 2011	Neuronal polarity
UAS-nSyb::GFP	M Ramaswami	Estes et al., 2000	Neuronal polarity
UAS-Syt::GFP UAS-DenMark::mCherry	BDSC 33065	Nicolaï et al., 2010	Neuronal polarity
10XUAS-IVS-mCD8::RFP, 13XLexAOp2-mCD8::GFP (X)	BDSC 32229	Pfeiffer et al., 2010	Double Reporter
UAS-CD4::spGFP1-10	K Scott	Gordon and Scott, 2009	GRASP
LexAop-CD4::spGFP11	K Scott	Gordon and Scott, 2009	GRASP
LexAOp2-IVS>stop>spGFP11::CD4::HA-T2A-Brp::mCherry (attP2), UAS-spGFP1-10::CD4, UAS-HRP::CD2	C-H Lee	Karuppudurai et al., 2014	Single cell GRASP
P{hsFLP}12 y w; CyO/Sco	BDSC 1929		Single cell GRASP
pBPhsFlp2::PEST(attP3); +; HA_V5_FLAG_OLLAS	M Landgraf	Nern et al., 2015	*Multicolor Flpout (MCFO-2)*
Tub84B(FRT-GAL80)1, w; Bl/CyO; TM2/TM6B	BDSC 38879		sVUM1 instersection
P{8xLexAop2-FLPL}attP40	B Pfeiffer, Janelia		sVUM1 instersection
UAS-Chrimson::mVenus (III)	BDSC 55136	Klapoetke et al., 2014	Effector/reporter for intersectional lines
y^1 w^*; +; Mi{MIC}Oamb^{MI12417}	BDSC 57940	Venken et al., 2011	Line for generating *Oamb::EGFP*
y^1 w^*; +; Mi{PT-GFSTF.1}Oamb$^{MI12417\text{-}GFSTF.1}$/TM6C	Fly Facility, Dept. of Genetics	This work	*Oamb::EGFP* line
Mi{MIC}Octβ1R^{MI05807}	BDSC 42119	Venken et al., 2011	Line for generating *Octβ1R::EGFP*
Mi{MIC}Octβ2R^{MI13416}	BDSC 59133	Venken et al., 2011	Line for generating *Octβ2R::EGFP*
Mi{MIC}Octβ2R^{MI06217}	BDSC 59133	Venken et al., 2011	Line for generating *Octβ3R::EGFP*
Mi{PT-GFSTF.2}Octβ1R$^{MI05807\text{-}GFSTF.2}$	Fly Facility, Dept. of Genetics	This work	*Octβ1R::EGFP line*
Mi{PT-GFSTF.2}Octβ2R$^{MI13416\text{-}GFSTF.2}$	Fly Facility, Dept. of Genetics	This work	*Octβ2R::EGFP line*
Mi{PT-GFSTF.0}Octβ3R$^{MI06217\text{-}GFSTF.0}$	Fly Facility, Dept. of Genetics	This work	*Octβ3R::EGFP line, GFP intron phase 0*
Mi{PT-GFSTF.1}Octβ3R$^{MI06217\text{-}GFSTF.1}$	BDSC 60245	Nagarkar-Jaiswal et al., 2015	*Octβ3R::EGFP line, GFP intron phase 1*

Table 2. Primers

Primer	Sequence	Purpose
MiMIC-5R	CTTGAGATTAAGGTAGCTTACGC	Verifying Mi{MIC} insertion
MiMIC-3F	TGCAGGTCGACGAATTCAAC	Verifying Mi{MIC} insertion
MI12417-5F	CCACAATCAACGTCCTGCTC	Verifying Mi{MIC} insertion
MI12417-3R	GATTATCGCCACCACAGAGTC	Verifying Mi{MIC} insertion
MI05807-5F	TCCTTTCATTCCCGAGCACC	Verifying Mi{MIC} insertion
MI05807-3R	CTCGTTAACAATCGCTCGCC	Verifying Mi{MIC} insertion
MI13416-5F1	CGGAGTCACTGAGTAATGGCG	Verifying Mi{MIC} insertion
MI13416-5F2	ATGGCGAGTGGTATGAGCAG	Verifying Mi{MIC} insertion
MI13416-5F3	GTGCTCTAGATGGCGAGTGG	Verifying Mi{MIC} insertion
MI13416-5F4	ACCGAGGCTCATTAACACAG	Verifying Mi{MIC} insertion
MI13416-5F5	GAGGCTCATTAACACAGCGC	Verifying Mi{MIC} insertion
MI13416-3R	GCTGCCTCATTGAACTCCAG	Verifying Mi{MIC} insertion
MI06217-5F	GCAGGAGAACAGCGACAGTC	Verifying Mi{MIC} insertion
MI06217-3R	CCTGTCTCTGGAAGTAGGTCG	Verifying Mi{MIC} insertion
Orientation-MiL-F (OriF)	GCGTAAGCTACCTTAATCTCAAGAAGAG	Verifying GFP swap orientation
Orientation-MiL-R (OriR)	CGCGGCGTAATGTGATTTACTATCATAC	Verifying GFP swap orientation
EGFPdo-Seq-F (EGFP-F)	GGATGACGGCACCTACAAGAC	Verifying GFP swap orientation
EGFPdo-Seq-R (EGFP-R)	GTGGCTGTTGAAGTTGTACTC	Verifying GFP swap orientation

Table 3. Antibodies

Antibody	Host	Source	Dilution	Experiment or Figures
Anti-GFP	Rat, monoclonal	Nacalai 440426 (Clone GF090R)	1:1000	GRASP (4B,C,D,E) UAS-CD8::GFP
Anti-GFP	Chicken, polyclonal	Abcam, Ab13970	1:1000/1:2000	Oamb::EGFP (6)
Anti-GFP	Rabbit, polyclonal	Invitrogen, A11122	1:1000/1:2000	
Anti-GFP	Rabbit, polyclonal	Abcam, Ab290	1:800	
Anti-DsRed	Rabbit, polyclonal	Clontech, 632496	1:1000	UAS-tdTom (3A), UAS-DenMark (3B,C) Brp::mCherry (5B,C,D) UAS-RFP (6A),
Anti-GABA	Rabbit, polyclonal	Sigma, A2052	1:1000	Figs. 3D, 4C
Anti-OA	Rabbit, polyclonal	MoBiTec, 1003GE	1:1000	Figs 4B,C,D,E
Anti-Dlg	Mouse, monoclonal	DSHB, 4F3	1:200	Figs. 3,4,5,6
Anti-FLAG	Mouse, monoclonal	Sigma, 1804	1:4000	MCFO
Anti-HA	Rat, monoclonal	Roche, 3F10	1:1000	MCFO (2A,B)
Anti-V5	Chicken, polyclonal	Abcam Ab1993	1:1000	MCFO (2A,B)
Secondary Antibody	**Host**	**Source**	**Dilution**	
Anti-Rat Alexa 488	Goat, polyclonal	Invitrogen, A11006	1:200	
Anti-Rat Alexa 594	Goat, polyclonal	Invitrogen, A11007	1:200	
Anti-Chicken Alexa 488	Goat, polyclonal	Invitrogen, A11039	1:200	
Anti-Rabbit Alexa 488	Goat, polyclonal	Invitrogen, A11034	1:200	
Anti-Rabbit Alexa 568	Goat, polyclonal	Invitrogen, A11036	1:200	
Anti-Mouse Alexa 647	Goat, polyclonal	Invitrogen, A21236	1:200	
Anti-Rabbit Alexa 647	Goat, polyclonal	Invitrogen, A21245	1:200	
Anti-Chicken Alexa 568	Goat, polyclonal	Invitrogen, A11041	1:200	

Supplementary Figure Legends

Supp Fig. 1. Expression of IT.GAL4 lines H275 and H300 in larval mushroom body. Panels show projections of confocal stacks of the genotypes shown. Most Kenyon cell bodies are not included, to avoid obscuring the rest of the MB.

Supp Fig 1

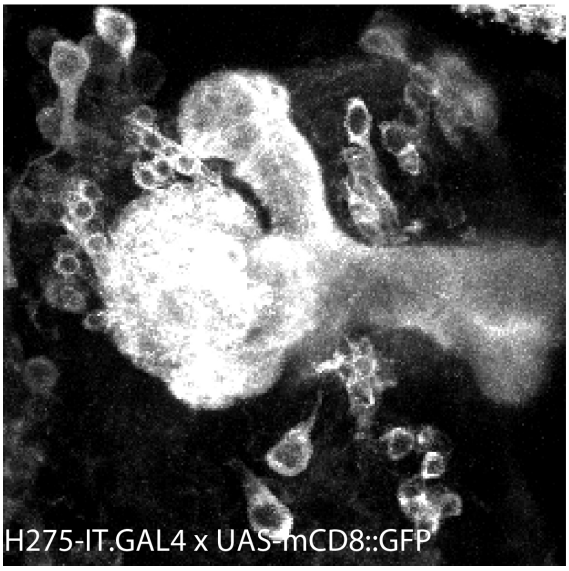

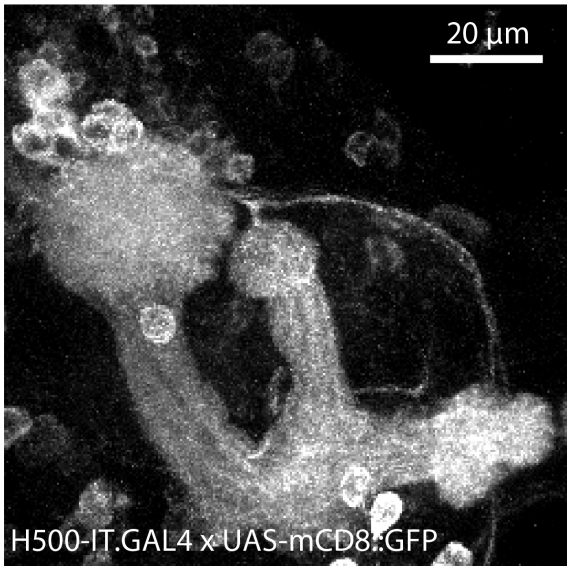

Supp Fig 2. PCR verification of *MI12417(Oamb)* insertion in the *Oamb* gene. (A) Primers designed against 5' (*MI12417-5F/MiMIC-5R*) and 3' (*MiMIC-3F/MI12417-3R*) *MiMIC* insertion flanking ends were used to validate the *MI12417* insertion in the *Oamb* gene. **(B)** PCR results for *MI12417* MiMIC insertion. PCR products were detected for *MI12417* 5' and 3' flanking ends using *MI12417* DNA template, but not for negative control template (denoted as +). A PCR product was detected using primers against the *Oamb* genomic flanking sequences (*MI12417-5F/MI12417-3R)* for the negative control lacking *MI12417* insertion, as well as for *MI12417* due to heterozygosity of the insertion. Abbreviations: MiL/MiR, *MiMIC* insertion ends Left/Right. SA, Splice Acceptor Site.

A

B

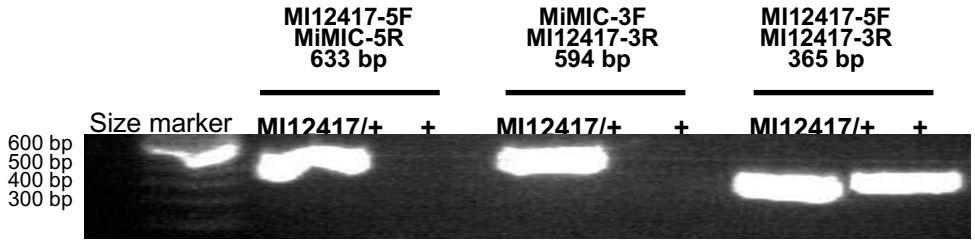

Supplementary Figure 3. Alignment of *MI12417* 5' flanking PCR products to MiMIC and Oamb genomic sequences. (A) Sequenced 5' *MI12417* PCR product. Alignment to MiMIC sequences is indicated in yellowa lignment to *Oamb* in grey. Overlapping alignment at the MiMIC insertion site (TA) indicated in red. **(B-C)** Alignment of *MI12417* 5' PCR products to MiMIC **(B)** and *Drosophila melanogaster* **(C)** sequences using Nucleotide BLAST (Altschul et al., 1990).

A. Sequence of *MI12417* 5' flanking end

```
NTCTTTATTCGCATAATATAAATCACATGGCTCAAAGAAGAAGTCACGCATCATAATTAG
CATTATATTCCAAGTTGGGCAAAAACAAGAAATCGATAAACGCTGAGGAAGCACATCAAA
CAAATCGGCTTAGATAAAATTGAGGTTGGGATTAAATAGGAGCGGGATTCCAGCCAGAAA
ATGGCAGACATGAAAGCGAGCCATCGGCTAAAACGAAATAAAATATACGAGCCCCAACCA
CTATTAATTCGAACAGCATGTTTTTTTGCAGTGCGCAATGTTTAACACACTATATTATCA
ATACTACTAAAGATAACACATACCAATGCATTTCGTCTCAAAGAGAATTTTATTCTCTTC
ACGACGAAAAAAAAAGTTTTGCTCTATTTCCAACAACAACAAAAATATGAGTAATTTATT
CAAACGGTTTGCTTAAGAGATAAGAAAAAAGTGACCACTATTAATTCGAACGCGGCGTAA
GCTACTAAATCTCTCANGAA
```

B. *MI12417* 5' flanking end alignment with *Oamb*

```
>AE014297.3 Drosophila melanogaster chromosome 3R      Length=32079331
Features in this part of subject sequence:
   octopamine receptor in mushroom bodies, isoform D
   octopamine receptor in mushroom bodies, isoform G

Strand=Plus/Minus
Query  71        CAAGTTGGGCAAAAACAAGAAATCGATAAACGCTGAGGAAGCACATCAAACAAATCGGCT  130
                 ||||||||||||||||||||||||||||||||||||||||||||||||||||||||||||
Sbjct  20697214  CAAGTTGGGCAAAAACAAGAAATCGATAAACGCTGAGGAAGCACATCAAACAAATCGGCT  20697155

Query  131       TAGATAAAATTGAGGTTGGGATTAAATAGGAGCGGGATTCCAGCCAGAAAATGGCAGACA  190
                 ||||||||||||||||||||||||||||||||||||||||||||||||||||||||||||
Sbjct  20697154  TAGATAAAATTGAGGTTGGGATTAAATAGGAGCGGGATTCCAGCCAGAAAATGGCAGACA  20697095

Query  191       TGAAAGCGAGCCATCGGCTAAAACGAAATAAAATATA  227
                 |||||||||||||||||||||||||||||||||||||
Sbjct  20697094  TGAAAGCGAGCCATCGGCTAAAACGAAATAAAATATA  20697058
```

C. *MI12417* 5' flanking end alignment with MiMIC sequences

```
>GU370067.1 Synthetic construct MIMIC transposable element, complete sequence   Length=7267

Strand=Plus/Plus
Query  226  TACGAGCCCCAACCACTATTAATTCGAACAGCATGtttttttGCAGTGCGCAATGTTTAA  285
            ||||||||||||||||||||||||||||||||||||||||||||||||||||||||||||
Sbjct  102  TACGAGCCCCAACCACTATTAATTCGAACAGCATGTTTTTTTGCAGTGCGCAATGTTTAA  161

Query  286  CACACTATATTATCAATACTACTAAAGATAACACATACCAATGCATTTCGTCTCAAAGAG  345
            ||||||||||||||||||||||||||||||||||||||||||||||||||||||||||||
Sbjct  162  CACACTATATTATCAATACTACTAAAGATAACACATACCAATGCATTTCGTCTCAAAGAG  221

Query  346  AATTTTATTCTCTTCACGACGaaaaaaaaaaGTTTTGCTCTATTTCCAACAACAACAAAAA  405
            ||||||||||||||||||||||||||||||||||||||||||||||||||||||||||||
Sbjct  222  AATTTTATTCTCTTCACGACGAAAAAAAAAAGTTTTGCTCTATTTCCAACAACAACAAAAA  281

Query  406  TATGAGTAATTTATTCAAACGGTTTGCTTAAGAGATAAGAAAAAAGTGACCACTATTAAT  465
            ||||||||||||||||||||||||||||||||||||||||||||||||||||||||||||
Sbjct  282  TATGAGTAATTTATTCAAACGGTTTGCTTAAGAGATAAGAAAAAAGTGACCACTATTAAT  341
```

Supplementary Figure 4. Alignment of 3' flanking PCR products from *MI12417* to MiMIC and Oamb genomic sequences (A) Sequenced 3' *MI12417* PCR product. Alignment to MiMIC sequences are indicated in yellow; while alignment to *Oamb* sequences are indicated in grey. Overlapping alignment at the MiMIC insertion site (TA) indicated in red. **(B-C)** Alignment of *MI12417* 3' PCR products to MiMIC **(B)** and *Drosophila melanogaster* **(C)** sequences using Nucleotide BLAST (Altschul et al., 1990).

A. Sequence of *MI12417* 3' flanking end

```
GCGGGAGTCGCGACTACGCCCCCACTGAGAGACTCAAAGGTTTACCCCAGTTGGGGCACT
ACTCCCGAAAACCGCTTCTGACCTGGGCCGCGGGGGAAATTAATTAAATTATTGTTTTAA
GTATGATAGTAAATCACATTACGCCGCGTTCGAATTAATAGTGGTCACTTTTTTCTTATC
TCTTAAGCAAACCGTTTGAATAAATTACTCATATTTTTGTTGTTGTTGGAAATAGAGCAA
AACTTTTTTTTTCGTCGTGAAGAGAATAAAATTCTCTTTGAGACGAAATGCATTGGTATG
TGTTATCTTTAGTAGTATTGATAATATAGTGTGTTAAACATTGCGCACTGCAAAAAAAAC
ATGCTGTTCGAATTAATAGTGGTTGGGGCTCGTAATATGTCTTCCCTGTTAGCATGTTCT
GTTTGCAATTTTCTATTTTCTTAGGTTTTTGTCGTTTCAGGCCTCACTGGTCCCCAAAGA
CTCTGTGGGGCCGGATAATCGGCTTTGTTCTGACAGCCGTTTTTTTGCTGGGCTGAATGT
TTAACACACTGGACCATCAGTTTGACTCAGGACTCACGGACCAGTGGCTCCTCCTCTCAA
AGAGAGTTTTATTCTCCTCGCCACAGCAAGGAAGGCCCTGCACGATGTCGAACAGGACCC
CGTGTGGCTCATCTCTTGCTTCTGTGGGAGGCAAGTCTAACCCAGTGTGACCTCCATGAA
GTCGAGAACAAGTAACTCAATCTCCCATCCCACCCTTATGCTGCGCCAGACCCGTGAGGA
GCCCACCTCCGGTGGACAC
```

B. *MI12417* 3' flanking end alignment with MiMIC sequences

```
>AE014297.3 Drosophila melanogaster chromosome 3R      Length=32079331
Features in this part of subject sequence:
   octopamine receptor in mushroom bodies, isoform D
   octopamine receptor in mushroom bodies, isoform G

>GU370067.1 Synthetic construct MIMIC transposable element, complete sequence   Length=7267
Strand=Plus/Plus
Query  252   tCGTCGTGAAGAGAATAAAATTCTCTTTGAGACGAAATGCATTGGTATGTGTTATCTTTA  311
             ||||||||||||||||||||||||||||||||||||||||||||||||||||||||||||
Sbjct  7062  TCGTCGTGAAGAGAATAAAATTCTCTTTGAGACGAAATGCATTGGTATGTGTTATCTTTA  7121

Query  312   GTAGTATTGATAATATAGTGTGTTAAACATTGCGCACTGCaaaaaaaaCATGCTGTTCGA  371
             ||||||||||||||||||||||||||||||||||||||||||||||||||||||||||||
Sbjct  7122  GTAGTATTGATAATATAGTGTGTTAAACATTGCGCACTGCAAAAAAAACATGCTGTTCGA  7181

Query  372   ATTAATAGTGGTTGGGGCTCGTA  394
             |||||||||||||||||||||||
Sbjct  7182  ATTAATAGTGGTTGGGGCTCGTA  7204
```

C. *MI12417* 3' flanking end alignment with *Oamb* sequences

```
>AE014297.3 Drosophila melanogaster chromosome 3R     Length=32079331
Features in this part of subject sequence:
   octopamine receptor in mushroom bodies, isoform D
   octopamine receptor in mushroom bodies, isoform G

Strand=Plus/Minus
Query  393       TAATATGTCTTCCCTGTTAGCATGTTCTGTTTGCAATTTTCTATTTTCTTAGGTTTTTGT  452
                 ||||||||||||||||||||||||||||||||||||||||||||||||||||||||||||
Sbjct  20697059  TAATATGTCTTCCCTGTTAGCATGTTCTGTTTGCAATTTTCTATTTTCTTAGGTTTTTGT  20697000

Query  453       CGTTTCAGGCCTCACTGGTCCCCAAAGACTCTGTGGGGCCGGATAATC  500
                 |||||||||||||||||||||||||||||| |||||| | || ||||||
Sbjct  20696999  CGTTTCAGGCCTCACTGGTCCCCAAAGACGCTGTGGTGGCG-ATAATC  20696953
```

Supp Fig. 5. *MI12417* is inserted in coding intron 3 of *Oamb*. (A) Extract of TBLASTN query of Oamb-B against the *Drosophila* genome assembly, showing an intron at coordinates 20693849–20698333, inserted at amino-acid residue 338 of Oamb-B. **(B)**. Extract of BLASTN search of *Oamb-B* RNA, showing a splice site between nucleotides 2007 and 2008. **(C)** Alignment of Oamb-B protein and Oamb-B RNA sequences around the third intron, highlighting residue G338 and the AGGG splice site in yellow. **(D)** Map of *MI12417* insertion (3R:20,697,059) relative to *Oamb* gene and transcripts (Adapted from GBrowse, www.flybase.org).

A

```
Oamb-B:       284 PWKCELTNDRGYVLYSALGSFYIPMFVMLFFYWRIYRAAVRTTRAINQGFKTTKG 338
                  PWKCELTNDRGYVLYSALGSFYIPMFVMLFFYWRIYRAAVRTTRAINQGFKTTKG
Genome: 20698497 PWKCELTNDRGYVLYSALGSFYIPMFVMLFFYWRIYRAAVRTTRAINQGFKTTKG 20698333

Oamb-B:       338 GSPRESGNNRVDESQLILRIHRGRPCSTPQRTPLSVHSMSSTLSVNSNGGGGGAVASGLG 397
                  GSPRESGNNRVDESQLILRIHRGRPCSTPQRTPLSVHSMSSTLSVNSNGGGGGAVASGLG
Genome: 20693849 GSPRESGNNRVDESQLILRIHRGRPCSTPQRTPLSVHSMSSTLSVNSNGGGGGAVASGLG 20693670
```

B

```
Oamb-B:      1964 TGAGAACGACGAGAGCCATCAACCAGGGCTTCAAGACCACCAAG 2007
                  ||||||||||||||||||||||||||||||||||||||||||||
Genome: 20698379 TGAGAACGACGAGAGCCATCAACCAGGGCTTCAAGACCACCAAG 20698332

Oamb-B:      2008 GGCAGTCCCCGCGAGTCGGGCAACAATCGAGTGGACGAGTCCCAGCTCATATTGCGCATT 2067
                  ||||||||||||||||||||||||||||||||||||||||||||||||||||||||||||
Genome: 20693849 GGCAGTCCCCGCGAGTCGGGCAACAATCGAGTGGACGAGTCCCAGCTCATATTGCGCATT 20693790
```

C

```
                                   Coding intron 3; 3R:20,697,059
                                   Exon 4>3R:20,693,848-20,692,947
     ATCAACCAGGGCTTCAAGACCACCAAGGGCAGTCCCCGCGAGTCGGGCAACAATCGAGTG
329  -I--N--Q--G--F--K--T--T--K--G--S--P--R--E--S--G--N--N--R--V-
```

D

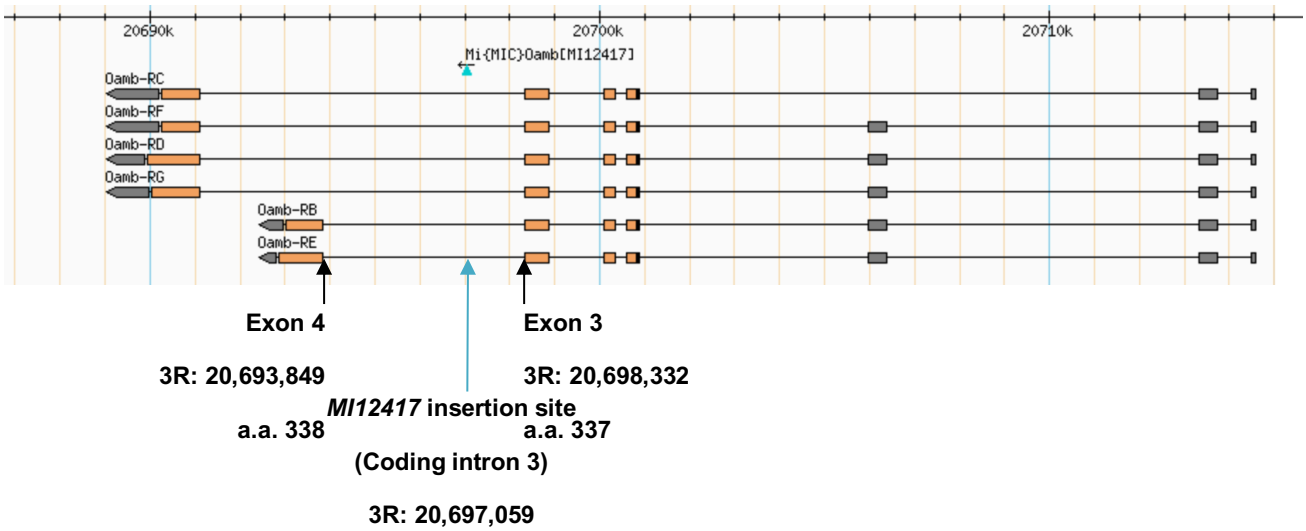

Supp. Fig. 6. TMHMM predictions of transmembrane domains for Oamb-PB and PC isotypes. The third intracellular loop, where residue G338 is found, is highlighted in yellow.

A. Oamb-PB TMHMM Predictions

WEBSEQUENCE	TMHMM2.0	outside	1	21
WEBSEQUENCE	TMHMM2.0	TMhelix	22	44
WEBSEQUENCE	TMHMM2.0	inside	45	56
WEBSEQUENCE	TMHMM2.0	TMhelix	57	79
WEBSEQUENCE	TMHMM2.0	outside	80	93
WEBSEQUENCE	TMHMM2.0	TMhelix	94	116
WEBSEQUENCE	TMHMM2.0	inside	117	136
WEBSEQUENCE	TMHMM2.0	TMhelix	137	159
WEBSEQUENCE	TMHMM2.0	outside	160	293
WEBSEQUENCE	TMHMM2.0	TMhelix	294	316
WEBSEQUENCE	TMHMM2.0	inside	317	523
WEBSEQUENCE	TMHMM2.0	TMhelix	524	546
WEBSEQUENCE	TMHMM2.0	outside	547	555
WEBSEQUENCE	TMHMM2.0	TMhelix	556	578
WEBSEQUENCE	TMHMM2.0	inside	579	637

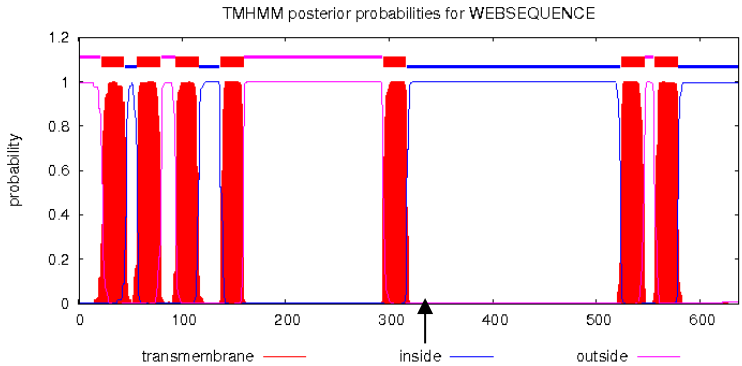

B. Oamb-PC TMHMM Predictions

WEBSEQUENCE	TMHMM2.0	outside	1	21
WEBSEQUENCE	TMHMM2.0	TMhelix	22	44
WEBSEQUENCE	TMHMM2.0	inside	45	56
WEBSEQUENCE	TMHMM2.0	TMhelix	57	79
WEBSEQUENCE	TMHMM2.0	outside	80	93
WEBSEQUENCE	TMHMM2.0	TMhelix	94	116
WEBSEQUENCE	TMHMM2.0	inside	117	136
WEBSEQUENCE	TMHMM2.0	TMhelix	137	159
WEBSEQUENCE	TMHMM2.0	outside	160	293
WEBSEQUENCE	TMHMM2.0	TMhelix	294	316
WEBSEQUENCE	TMHMM2.0	inside	317	520
WEBSEQUENCE	TMHMM2.0	TMhelix	521	543
WEBSEQUENCE	TMHMM2.0	outside	544	552
WEBSEQUENCE	TMHMM2.0	TMhelix	553	575
WEBSEQUENCE	TMHMM2.0	inside	576	645

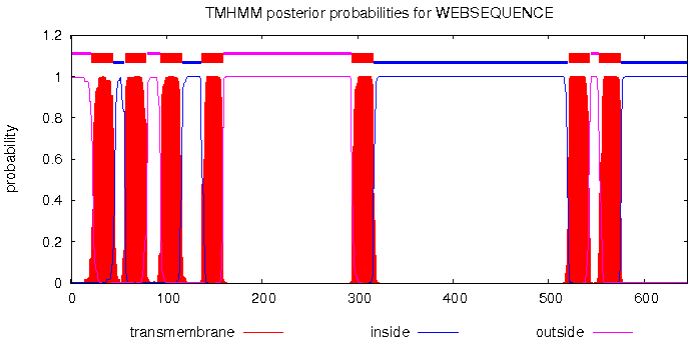

Supp. Fig. 7. *MI12417* insertion location relative to *Oamb* cDNA and protein sequences. cDNA and protein sequences were taken from the ENSEMBL database (Aken et al., 2016; http://www.ensembl.org) for representative *Oamb* transcript protein isotype B. The beginning and range of each exon, obtained from the ENSEMBL database, is annotated in yellow. Transmembrane domains are indicated in green. MiMIC insertion location site, listed on the Gene Disruption Project database, is annotated in light blue. Abbreviations: TM, transmembrane domain; a.a., amino acid

```
3R:20,700,845
Exon 1>3R:20,700,845-20,700,594
    1  ATGAATGAAACAGAGTGCGAGGAT
    1  -M--N--E--T--E--C--E--D-
                                                TM I: a.a.22-44
   25 CTCATCAAATCTGTGAAATGGACGGAACCAGCCAATCTGATCTCCCTGGCCGTACTCGAG
    9 -L--I--K--S--V--K--W--T--E--P--A--N--L--I--S--L--A--V--L--E-

   85 TTCATCAACGTTCTGGTCATCGGTGGCAACTGCCTCGTGATTGCCGCCGTCTTCTGTTCG
   29 -F--I--N--V--L--V--I--G--G--N--C--L--V--I--A--A--V--F--C--S-

                                TM II: a.a.57-79
  145 AATAAGTTGAGGAGTGTGACGAACTTCTTTATTGTCAACCTAGCTGTGGCCGATCTTCTG
   49 -N--K--L--R--S--V--T--N--F--F--I--V--N--L--A--V--A--D--L--L-

                                                        Exon 2>3R:20,700,331
  205 GTGGGTTTGGCCGTCCTACCCTTCTCAGCCACCTGGGAAGTCTTCAAGGTTTGGATATTC
   69 -V--G--L--A--V--L--P--F--S--A--T--W--E--V--F--K--V--W--I--F-

     -20,700,095        TM III: a.a.94-116
  265 GGCGATCTCTGGTGCCGCATTTGGCTGGCTGTCGATGTCTGGATGTGCACGGCATCGATC
   89 -G--D--L--W--C--R--I--W--L--A--V--D--V--W--M--C--T--A--S--I-

  325 CTGAATCTGTGTGCCATATCACTGGACCGCTATGTGGCGGTCACACGACCCGTCACCTAC
  109 -L--N--L--C--A--I--S--L--D--R--Y--V--A--V--T--R--P--V--T--Y-

                                TM IV: a.a.137-159
  385 CCAAGCATAATGTCCACGAAGAAGGCCAAGTCCTTAATCGCCGGCATTTGGGTACTCTCA
  129 -P--S--I--M--S--T--K--K--A--K--S--L--I--A--G--I--W--V--L--S-

                                                      Exon 3>3R:20,698,857-
  445 TTTTTTATTTGCTTTCCGCCGCTAGTCGGCTGGAAGGATCAAAAGGCGGTTATACAGCCG
  149 -F--F--I--C--F--P--P--L--V--G--W--K--D--Q--K--A--V--I--Q--P-

      20,698,335
  505 ACCTATCCAAAGGGAAACCATACGCTTTACTACACCACCACGATGTCAAGCTCGGAGGAT
  169 -T--Y--P--K--G--N--H--T--L--Y--Y--T--T--T--M--S--S--S--E--D-

  565 GGTCAACTAGGGTTAGATAGCATTAAGGACCAGGGCGAGGCATCCTTGCCTCCATCCCCG
  189 -G--Q--L--G--L--D--S--I--K--D--Q--G--E--A--S--L--P--P--S--P-

  625 CCCCATATCGGCAACGGCAACGCCTACAATCCCTACGATCCCGGTTTCGCACCCATCGAT
  209 -P--H--I--G--N--G--N--A--Y--N--P--Y--D--P--G--F--A--P--I--D-

  685 GGATCCGCGGAGATTCGGATTGCGGCCATTGACTCGACCAGTACTTCAACAACCGCAACC
  229 -G--S--A--E--I--R--I--A--A--I--D--S--T--S--T--S--T--T--A--T-

  745 ACCACGACGACAGCGTCCAGCTCGAGCACCACGGAAACGGAAATGGACCTCGATCTACTG
  249 -T--T--T--T--A--S--S--S--S--T--T--E--T--E--M--D--L--D--L--L-

  805 AACGCACCGCCGCAGAACAGACCCCAAACAATTTCCGGCAGTTGTCCGTGGAAGTGCGAG
  269 -N--A--P--P--Q--N--R--P--Q--T--I--S--G--S--C--P--W--K--C--E-
```

```
                    TM V: a.a.294-316
 865 CTGACCAACGATCGGGGTTATGTCCTGTACTCCGCCCTGGGCTCATTCTATATACCCATG
 289 -L--T--N--D--R--G--Y--V--L--Y--S--A--L--G--S--F--Y--I--P--M-

 925 TTCGTGATGCTCTTCTTCTACTGGCGCATCTACCGGGCTGCCGTGAGAACGACGAGAGCC
 309 -F--V--M--L--F--F--Y--W--R--I--Y--R--A--A--V--R--T--T--R--A-

                                MI12417> Coding intron 3; 3R:20,697,059
                                          MI12417> Intracellular: a.a.338
                                Exon 4>3R:20,693,848-20,692,947
 985 ATCAACCAGGGCTTCAAGACCACCAAGGGCAGTCCCCGCGAGTCGGGCAACAATCGAGTG
 329 -I--N--Q--G--F--K--T--T--K--G--S--P--R--E--S--G--N--N--R--V-

1045 GACGAGTCCCAGCTCATATTGCGCATTCACCGAGGAAGACCTTGCTCCACCCCCCAGCGC
 349 -D--E--S--Q--L--I--L--R--I--H--R--G--R--P--C--S--T--P--Q--R-

1105 ACGCCCCTCTCGGTGCACTCAATGTCCTCGACTCTCAGCGTGAACAGCAACGGGGGCGGG
 369 -T--P--L--S--V--H--S--M--S--S--T--L--S--V--N--S--N--G--G--G-

1165 GGTGGAGCCGTGGCCTCGGGACTGGGTGCCTCCACCGAGGATCACCTTCAGGGAGGCGCC
 389 -G--G--A--V--A--S--G--L--G--A--S--T--E--D--H--L--Q--G--G--A-

1225 CCCAAGCGGGCCACATCGATGCGCGTCTGCCGACAGCGACACGAGAAGGTGGCCATCAAG
 409 -P--K--R--A--T--S--M--R--V--C--R--Q--R--H--E--K--V--A--I--K-

1285 GTGTCCTTTCCCTCCTCCGAGAATGTCCTCGACGCAGGACAGCAGCCACAGGCATCGCCA
 429 -V--S--F--P--S--S--E--N--V--L--D--A--G--Q--Q--P--Q--A--S--P-

1345 CACTATGCGGTAATCAGTAGCGCCAACGGACGTCGTGCCTCCTTTAAGACGAGCCTCTTC
 449 -H--Y--A--V--I--S--S--A--N--G--R--R--A--S--F--K--T--S--L--F-

1405 GACATTGGCGAGACCACCTTTAATTTGGACGCAGCTGCGTCCGGTCCCGGAGACCTAGAG
 469 -D--I--G--E--T--T--F--N--L--D--A--A--A--S--G--P--G--D--L--E-

1465 ACCGGACTCTCGACCACCTCACTGTCGGCCAAGAAGCGGGCAGGCAAGCGCAGCGCCAAG
 489 -T--G--L--S--T--T--S--L--S--A--K--K--R--A--G--K--R--S--A--K-

                                                    TM VI: a.a.524-546
1525 TTTCAGGTGAAGCGGTTCCGAATGGAGACCAAGGCAGCCAAGACGCTGGCCATCATTGTG
 509 -F--Q--V--K--R--F--R--M--E--T--K--A--A--K--T--L--A--I--I--V-

1585 GGCGGCTTCATCGTTTGCTGGCTGCCCTTCTTCACGATGTATCTGATCCGGGCCTTCTGC
 529 -G--G--F--I--V--C--W--L--P--F--F--T--M--Y--L--I--R--A--F--C-

                          TM VII: a.a.556-578
1645 GACCACTGCATTCAGCCGACGGTCTTTTCGGTGCTCTTCTGGCTGGGCTACTGCAACTCG
 549 -D--H--C--I--Q--P--T--V--F--S--V--L--F--W--L--G--Y--C--N--S-

1705 GCCATTAATCCGATGATCTATGCGCTCTTCTCGAATGAGTTTCGCATCGCCTTCAAGCGG
 569 -A--I--N--P--M--I--Y--A--L--F--S--N--E--F--R--I--A--F--K--R-

1765 ATAGTGTGCAGATGCGTCTGCACCCGCAGTGGCTTCCGGGCGTCGGAGAATTTCCAGATG
 589 -I--V--C--R--C--V--C--T--R--S--G--F--R--A--S--E--N--F--Q--M-

1825 ATAGCGGCGCGTGCCCTGATGGCACCGGCAACATTCCACAAGACCATATCCGGATGCTCG
 609 -I--A--A--R--A--L--M--A--P--A--T--F--H--K--T--I--S--G--C--S-

1885 GACGACGGCGAGGGCGTGGACTTCAGCTGA
 629 -D--D--G--E--G--V--D--F--S--*-
```